QUANTUM THEORY OF INTERSTITIAL DIFFUSION

by Henrik Stenlund

A Private Study

Revision History:
10-10-2003 one missing page was added

ABSTRACT

A quantum theory of atomic diffusion in solids is presented and applied to a particular problem of interstitial diffusion, Li in Ge and Si. The theory is based on transport in allowed narrow bands using the relaxation time approximation. The bands were calculated by using a proper potential model through numerical methods. The relaxation time was taken from the theory of Kagan and Klinger [18] and the diffusion coefficients were calculated. For comparison the result of the theory of Kagan and Klinger for the diffusion coefficient was put also in numerical form. All coefficients show relatively good agreement with experimental values (see table 3.). The isotopic effect was also studied and D_o and E_o were found to have dependences $m^{-\frac{1}{2}}$ and $A \cdot m^{-1} + B$ respectively.

CONTENTS

2 INTRODUCTION

a. Introductory theory

An excess atom brought into solvent lattice finds itself located in an equilibrium site between the lattice atoms and vibrates about the site as the others do. At high temperatures it may randomly jump to the neighbouring free equilibrium site (see figure 1.), from which it can again move to another site. The interstitial atom may jump in one of 10^3 to 10^5 vibrations when it has received energy enough from the lattice in form of thermal excitations, phonons, to exceed the potential barrier separating the equilibrium sites.

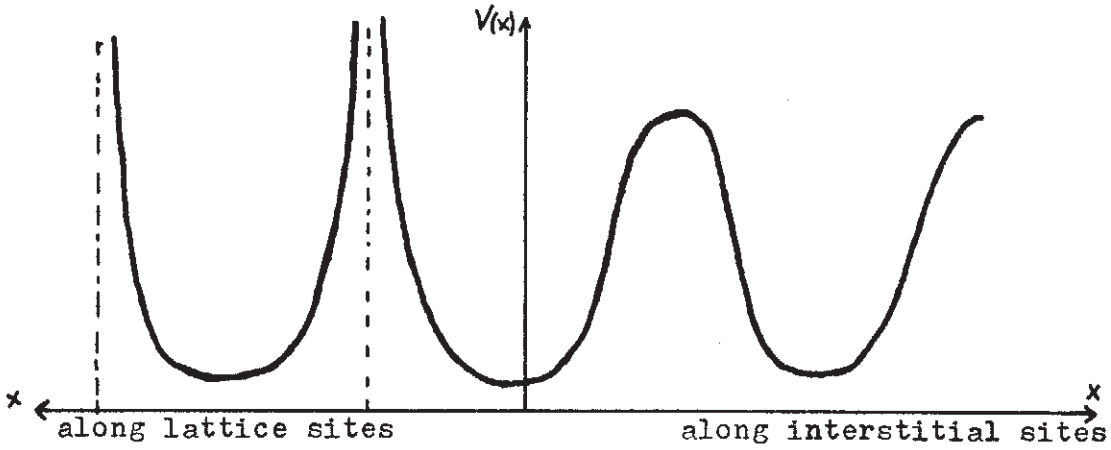

Figure 1. The lattice potential

The transitions between vibrational energy levels are usually connected with successive single-phonon processes (thus becoming a multi-phonon process) due to the large gaps between levels prohibiting single phonon transitions. The equilibrium

distribution for interstitial atoms among their allowed energies is Boltzmann's classical distribution giving strong dominance to the lowest level and only a small fraction occupies the overbarrier levels. There is another phenomenon assisting the jump and it is due to the fluctuations of the surrounding atoms opening the barrier and making it easier for the atom to move. This is significant only for large interstitial atoms, whose ion cores are of so large radius that they are even from a geometrical standpoint prevented from moving.

From these random jumps it follows that the excess atom diffuses in the lattice by an interstitial mechanism. There are, of course, several other mechanisms causing mass transport in lattice and of these we can mention one of the most noteworthy, the vacancy mechanism. By it we mean a solute atom-solvent lattice vacancy pair moving together. The solute atom has substituted one lattice atom and the vacancy moves around the solute. This motion is, of course, due to the jumping of solvent atoms to the vacancy thus leaving vacancies behind them (see fig.2. below). Only as the solute atom jumps to the vacancy is diffusion brought about and thus the pair is strongly correlated in its motion. Vacancies are very common at high temperatures being formed by thermal excitations. The vacancy mechanism is dominating in self-diffusion and for some elements in solute diffusion in semiconductors. In this work

Figure 2.

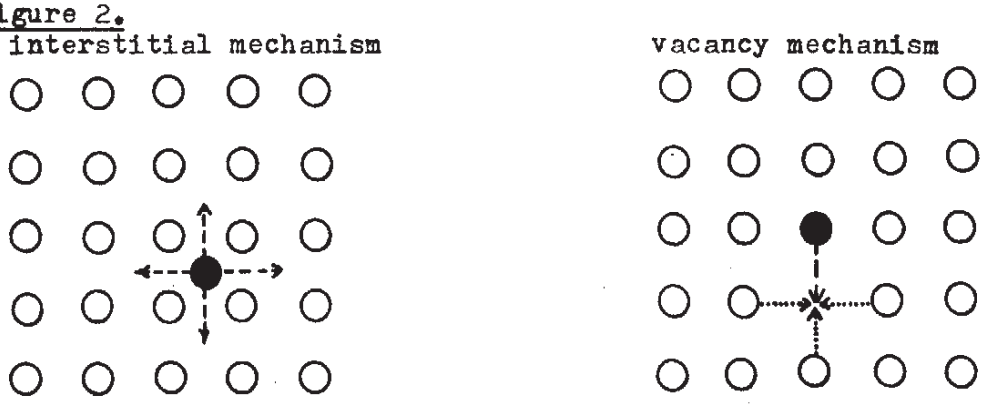

diffusion by interstitial mechanism only is studied but the theory can usually be directly applied to other mechanisms.

Experimentally one has observed an interesting behaviour for the diffusion coefficient as a function of temperature, mostly at high temperatures

$$D = D_o \, e^{-U_o/kT}, \qquad (1)$$

where U_o is the potential barrier height and D_o is independent of T. This is called Arrhenius' equation and D obeys it very well in almost all mass transport through solids. It is clear that the nature of the dependence derives its origin from the factor of Boltzmann for occupation as we shall later see.

In the following two sections we will shortly rewiev some existing approaches in calculating D for particles in crystals considering both classical and quantum theories.

b. Classical theories

The first theory explaining the Arrhenius-type behaviour of $D(\beta)$ was the Absolute Reaction Rate Theory due to Glasstone et al. [1] using the concept of transition state in one dimension. They considered the activated state, which is produced at the moment the particle is in the region of the saddle point, to consist of similar energy levels as the normal state around the equilibrium point (see fig. 3.). From this they concluded by statistical arguments that the jump rate Γ had to be a product of the concentration (fraction $c_\ddagger$) of the particles in the activated state and the mean velocity of the same particles in the direction of the irreversible jump divided by the width of the activated state

$$\Gamma = c_\ddagger' \frac{\bar{v}}{\delta} = c_\ddagger \frac{kT}{h}. \qquad (2)$$

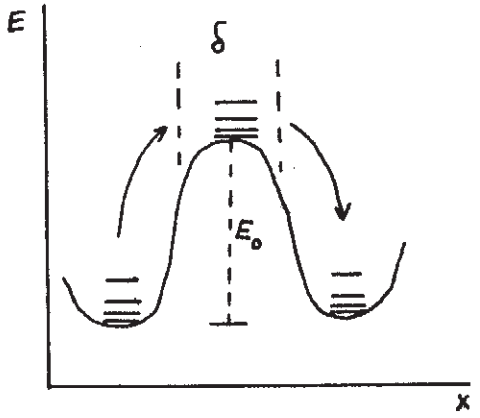

Figure 3. The activated state

They obtained for the concentration the ratio between the partition functions of the activated state and the normal state and as a result of re-normalization of energy zeros the factor $e^{-\beta E_0}$ appeared

$$D = \lambda^2 \frac{kT}{h} \frac{F_\ddagger}{F} e^{-\beta E_0}, \qquad (3)$$

where $F_\ddagger$ is the partition function belonging to the activated state (energy normalized) and F is the one in the normal state and λ is the jump distance.

The principal assumption is that the particle is moving isothermally and reversibly from one equilibrium site to another along

the reaction coordinate. The moving particle is considered to be in thermal equilibrium with the lattice at all times.

Wert and Zener [2] and Zener [3] developed the rate theory further to accomodate to the requirements of solid state diffusion and they obtained for the jump frequency Γ

$$\Gamma = n\bar{\nu}\, e^{-\Delta G^*/kT} = n\bar{\nu}\, e^{\Delta S^*/k}\, e^{-\Delta H^*/kT}. \qquad (4)$$

Here n is the number of ways available for the particle to move from site to site and $\bar{\nu}$ is the vibrational frequency of the particle in the initial state. ΔG^*, ΔS^* and ΔH^* represent the isothermal work associated with the motion of the particle to the activated state and changes of entropy and enthalpy respectively. When this expression is substituted into the basic equation for D in the random walk theory, we have (see Chandrasekhar [7])

$$D = \frac{\lambda^2 n \bar{\nu}}{6}\, e^{\Delta S^*/k}\, e^{-\Delta H^*/kT}. \qquad (5)$$

The basic assumptions of this theory have not been proved to be valid and it is difficult to believe that the motion of the particle would be reversible and the lifetime of the activated state could be long enough to allow the use of equilibrium statistical mechanics. The value of $\bar{\nu}$ is not clearly defined in this theory and is usually put equal to the Debye or Einstein frequency without giving any reason for its applicability.

An attempt to improve the definition of $\bar{\nu}$ was made by Wert [4], who used classical statistical methods to evaluate the jump rate and calculated $\bar{\nu}$ using the assumption of small harmonic vibrations around the equilibrium point.

Vineyard [5] derived a more general approach to calculate Γ avoiding thermodynamics. His theory gave the jump rate as a ratio of probabilities of all points on the saddle surface (in configuration space), which have positive velocities towards the diffusion direction to the sum of all points in configuration space around the initial equilibrium site. Thus Vineyard obtains

$$\Gamma = n\sqrt{\frac{kT}{2\pi}}\,\frac{\int_S e^{-\phi/kT}\,dS}{\int_V e^{-\phi/kT}\,dV}\,, \qquad (6)$$

where ϕ is the potential energy. This is essentially a ratio of two configurational partition functions. Employing the theory of small vibrations Vineyard expanded the potential around the extremal points and neglected terms of higher order than harmonic. His result for Γ was

$$\Gamma \simeq \frac{n\prod_{i=1}^{3N}\nu_i\; e^{-\Delta G'/kT}}{\prod_{i=1}^{3N-1}\nu_i'}\,, \qquad (7)$$

where ν_i are the 3N normal frequencies of atoms in their equilibrium states and ν_i' are the 3N-1 normal frequencies associated with the activated complex. $\Delta G'$ is the free energy difference between the initial site and the saddle point.

It is readily realized that this theory contains many crucial hypotheses, which limit the validity of the theory. Vineyard's Γ is based upon the assumption that an activated state exists and that when an atom passes over the potential barrier the probability of reversing the direction is vanishingly small.

The advantages of Vineyard's theory over Absolute Reaction Reaction Rate Theory are that the frequencies are defined in terms

of the solvent lattice normal frequencies in the normal state and in saddlepoint configuration but finally the calculation of $\bar{\nu}$ is still not well defined (in fact it is almost incalculable in Vineyard's theory).

Rice [6] has avoided the use of equilibrium statistical mechanics in his dynamical theory by using a normal mode analysis in the harmonic approximation. Rice calculated the frequency of occurrence $P(\{\delta\})$ of the appropriate configuration in which the diffusing atom has a large enough vibration amplitude to diffuse in the right direction and the surrounding atoms are appropriately in an out-of-phase motion giving

$$\Gamma = n \sum \frac{[V]}{S} P(\{\delta\}), \tag{8}$$

where

$$P(\{\delta\}) = \bar{\nu}\, e^{-U_0/kT} \prod_j e^{-U_j/kT} \prod_{k>l} g_{kl}^{(2)}. \tag{9}$$

Here $\bar{\nu}$ is some weighted mean frequency and U_0 is the critical energy needed for the atoms to reach the proper amplitude and U_j is the energy required to shift the barrier atoms in the lattice from their equilibrium positions and $g_{kl}^{(2)}$ is the pair correlation function for atoms k and l. $[V]$ and S stand for the concentrations of vacancies and solvent lattice atoms respectively.

Although this theory has been derived for diffusion by the vacancy mechanism, it is directly applicable to other mechanisms, e.g. to interstitial mechanism. The equation for Γ is very general and in order to obtain calculable expressions simplifying assumptions are to be made. Clearly the critical amplitude must be at least one-

half the jump distance (small frequency oscillation) and the oscillators must be harmonic. The number of normal modes associated with the process of achieving a critical amplitude is essentially smaller than the total number of modes of the crystal. Finally the frequency of thermal fluctuations around the diffusing atom is much greater than the jump rate.

Rice obtained for the pair correlation function in terms of the potential W_{kl} between atoms k and l

$$g_{kl}^{(2)} = e^{-W_{kl}/kT} \quad , \quad W_{kl} = \Delta H_{kl} - T\Delta S_{kl} \tag{10}$$

and Γ becomes

$$\Gamma = n\bar{\nu}\, e^{\sum_{k>l} \Delta S_{kl}/k}\, e^{-(U_0 + \sum_j U_j + \sum \Delta H_{kl})/kT}. \tag{11}$$

In this equation we can identify the term

$$\Delta H^k = U_0 + \sum_j U_j + \sum_{k>l} \Delta H_{kl} \tag{12}$$

as the activation enthalpy of the rate theory.

The main weakness of Rice's theory is the assumption of harmonicity and to obtain better correlation with experimental data, anharmonic terms must be included. Rice's theory gives a many-body approach to the problem and it is in this respect closer to real processes than rate theories although it contains too many incalculable frequencies.

Glyde [8] calculated the jump rate by using first a dynamical method and then a purely statistical one making a kind of synthesis

of Vineyard's and Rice's theories showing their equivalence. The dynamical part uses classical mechanics in normal coordinates and Glyde calculates correlation functions with the aid of normal frequencies. Through calculation of fluctuations Glyde arrived at the jump frequency. By a statistical mechanical derivation he calculated the same fluctuations and similar expressions for Γ but by using different random variable theorems than Rice to obtain the probability of a fluctuation. Glyde's results are applicable when the force constants are known, although the frequencies must be in some way approximated to obtain numerical results from the expressions. Glyde's approach is without any doubt one of the best classical treatments for the diffusion coefficient.

Nardelli and Reatto [9] studied interstitial diffusion by Kubo's formalism starting from the Liouville equation for the total system and derived the evolution equation for a particle in a periodic potential. They coupled the equation to lattice vibrations in thermal equilibrium and obtained the expression for the diffusion coefficient of ionized impurities in silicon and germanium in good agreement with the experimental data

$$D = D_o e^{-U_o/kT} \tag{13}$$

$$D_o = C_L Z^{-2} kT \sqrt{U_o/2m} \tag{14}$$

$$C_L = 2 \mathcal{J} 4^4 3^{-10/3} \pi^{-2/3} \frac{r_o^6 \epsilon_o^2 \delta \quad C_L^2}{Z_L^2 e^4 \left(1 + 2\left(\frac{C_L}{C_t}\right)^2\right)}, \tag{15}$$

where the Z's are effective valences and $\mathcal{J}$ is a numerical factor equal to 0.525. r_o is the nearest neighbour distance, δ is the

mass density and the c's are the familiar sound velocities.

In all of these classical theories the isotopic mass dependence of D_o is $m^{-\frac{1}{2}}$, which is typical for all classical theories. Usually they do not show any mass dependence in activation energy.

c. Quantum theories

One of the first papers devoted to the quantum mechanical diffusion of massive particles in solids was by Gosar [10] . He studied the interstitial diffusion using a temperature dependent Green's function method taking into account the interaction between phonons and impurity atoms. However, Gosar's model for the ion-lattice interaction was much too simple to correspond to real solids because he used a one-dimensional model with harmonic wells and his quantum states were those of a harmonic oscillator. Gosar recognized the existence of allowed energy bands, whose widths he evaluated employing the WKB-method obtaining for the band (s)

$$\Delta \epsilon(s) = \frac{\pi}{2 l(s)} \sqrt{\frac{\xi(s) - U}{2m}}, \qquad (16)$$

where $\xi(s)$ is the energy of the bottom of the band and U is the height of the potential barrier. l(s) is approximately equal to the width of the potential barrier between two interstitial cavities.

Andreev and Lifshitz [11] studied the motion of crystal defects, impurities and vacancies, quantum mechanically in a periodic lattice at low temperatures showing that they move practically freely through the crystal. They exhibited the temperature dependence of the diffusion coefficient from low temperatures, where band motion is predominating, to intermediate temperatures, where D suffers a minimum because of interactions with phonons, up to high temperatures, where the activation type exponential is pre-

valent (classical diffusion).

At the time of publication of their study several papers appeared, where the motion of impurities or vacancies (defectons) were examined quantum mechanically (e.g. [12], [13], [14] and [15]). To these papers belongs one by Flynn and Stoneham [16]. They considered the motion as hopping between localized eigenstates ϕ_p of the particle using perturbation theory. In their approach the saddlepoint itself played no important role, only the localized initial and final state wave functions were relevant. Naturally the overlap between these states in the saddlepoint region is the principal factor in determining the hopping probability.

They calculated the hopping probabilities in terms of the matrix elements $J_{pp'}$ of the interaction potential between the ion and the lattice

$$W_{pp'} = \frac{|J_{pp'}|}{\hbar^2}\int_{-t}^{t} d\xi \exp\left\{\sum_{\bar{q}} \frac{\omega_{\bar{q}}^2 |\Delta Q_{\bar{q}}|^2}{2\hbar\,\omega_{\bar{q}}}\left[(2n_{\bar{q}}+1)(\cos\omega_{\bar{q}}\xi - 1) + i\sin\omega_{\bar{q}}\xi\right]\right\}. \qquad (17)$$

Here $J_{pp'} = \langle\phi_p|\mathcal{H}_{int}|\phi_{p'}\rangle$ and $\omega_{\bar{q}}$ are the normal frequencies of the lattice and $n_{\bar{q}}$ corresponds to the phonon occupation numbers. The $\Delta Q_{\bar{q}}$ are equal to the changes of the normal-mode (mass-weighted) coordinates of the lattice.

Flynn and Stoneham approximated this integral to obtain different expressions for the high- and low-temperature regions. The preceding result was derived under the assumption that $J_{pp'}$ is independent of the lattice configuration and therefore they also calculated, in the latter part of their work, the role of lattice-activated

processes. In lattice-activated diffusion the interstitial atom moves unhindered as the surrounding atoms fluctuate to "open" the barrier. In this case the potential barrier and the activation energy respectively can be very low. The theory of Flynn and Stoneham still leaves open the nature of localized states, which is difficult to determine and is strongly dependent on ion-lattice interaction.

After the investigation of Flynn and Stoneham a series of papers appeared devoted to studying the motion of defects in crystals, mainly vacancies and interstitial impurities. Of these we can mention Kagan and Maksimov [17], Kagan and Klinger [18] and Klinger [19].

Kagan and Maksimov [17] explored quantum diffusion in extremely narrow bands, whose widths $\Delta\epsilon$ are small compared with typical phonon frequencies. They derived an equation of motion for the density matrix including the interaction with phonons. Starting from the standard equation for the density matrix ρ

$$i\frac{\partial}{\partial t}\rho = \frac{1}{\hbar}[H,\rho], \qquad (18)$$

where $H = H_1^{\bullet} + H_2 + H'$ and $H_1^{\bullet}$ is the Hamiltonian of the particle in the periodic potential, H_2 is the Hamiltonian of the phonon subsystem and H' is the Hamiltonian of the particle phonon interaction. Using the particle density matrix $\rho_1 = \mathrm{Tr}\rho$ and $V = H' - \langle H \rangle$ they transformed the differential equation to an integral equation and finally obtained in the site representation a differential equation

$$\frac{\partial}{\partial t}\rho_{1\,\bar{m},\bar{n}} + \frac{i}{\hbar}[H_1,\rho_1]_{\bar{m},\bar{n}} = -I_{\bar{m},\bar{n}}, \qquad (19)$$

where

$$I_{\bar{m},\bar{n}} = \frac{\pi}{\hbar^2} \sum \rho_{2\alpha}^{(0)} \delta_\gamma (E_\alpha - E_\beta) \left\{ V_{\bar{m}\bar{s}}^{\alpha\beta} V_{\bar{s}\bar{l}}^{\rho\alpha} \rho_{1\bar{l}\bar{n}} + V_{\bar{l}\bar{s}}^{\alpha\beta} V_{\bar{s}\bar{n}}^{\beta\rho} \rho_{1\bar{m}\bar{l}} - 2 V_{\bar{m}\bar{s}}^{\alpha\beta} V_{\bar{l}\bar{n}}^{\beta\alpha} \rho_{1\bar{s}\bar{l}} \right\}. \tag{20}$$

Here $V_{\bar{m}\bar{s}}^{\alpha\rho}$ means a double matrix element with respect to phonon states α,ρ and localized states centered around sites $\bar{m}$ and $\bar{s}$ respectively. The function $\delta_\gamma(x)$ is defined as

$$\delta_\gamma(x) = \frac{1}{\pi} \left(\frac{\gamma}{x^2+\gamma^2} \right). \tag{21}$$

γ equals

$$2\pi \sum_{\rho',\beta} \left\langle |V_{\rho'\rho}^{\beta\alpha}|^2 \cdot \delta(E_\alpha - E_\beta) \right\rangle \tag{22}$$

and E_α is a phonon energy.

One of the basic assumptions in deriving this equation was that the characteristic time within which the density matrix ρ_1 changes ($10^{-7}...10^{-12}$ s) is large compared with all the characteristic interaction times ($\ll 10^{-15}$ s). Recognizing that the off-diagonal matrix elements of V in the site representation are very small they obtained

$$I_{\bar{m}\bar{n}}^{(0)} = \Omega_{\bar{m}\bar{n}} \rho_{1\bar{m}\bar{n}} \tag{23}$$

$$\Omega_{\bar{m}\bar{n}} = \frac{\pi}{\hbar^2} \sum \rho_{2\alpha}^{(0)} \delta_\gamma (E_\alpha - E_\beta) \left\{ V_{\bar{m}\bar{m}}^{\alpha\beta} V_{\bar{m}\bar{m}}^{\beta\alpha} + V_{\bar{n}\bar{n}}^{\alpha\beta} V_{\bar{n}\bar{n}}^{\rho\alpha} - 2 V_{\bar{m}\bar{m}}^{\alpha\beta} V_{\bar{n}\bar{n}}^{\beta\alpha} \right\}, \tag{24}$$

where $\rho_{2\alpha}^{(0)}$ is the phonon equilibrium density matrix, because we can

clearly assume that the phonons are in equilibrium with the impurity atom. $I_{\bar{m}\bar{n}}$ describes a kind of a collision integral and determines the attenuation of the off-diagonal elements. Clearly $\Omega_{\bar{m}\bar{n}}$ determined by the intrasite scattering has nothing to do with the overlap between the states of the neighbouring sites. Because $\Omega_{\bar{m}\bar{m}} = 0$, $I_{\bar{m}\bar{n}}$ has to be calculated more accurately to second order, as was done in [17]

$$I^{(2)}_{\bar{m}\bar{m}} = \frac{2\pi}{\hbar^2}\sum \rho^{(0)}_{2\alpha}\,\delta_\gamma(E_\alpha - E_\beta)\,|V_{\bar{m}\bar{s}}|^2\,(\rho_{1\,\bar{m}\bar{m}} - \rho_{1\,\bar{s}\bar{s}})\,. \qquad (25)$$

This gives the attenuation factor for the diagonal elements of the density matrix corresponding to intersite scattering in noncoherent tunneling. Approximating further these expressions Kagan and Maksimov obtained finally for D

$$D = D_{coh} + D_{incoh}\,, \qquad (26)$$

where

$$D_{coh} = \frac{h^2 a^2 z}{3\,\Omega_1} \qquad (27)$$

$$D_{incoh} = \frac{\pi z a^2}{3}\sum \rho^{(0)}_{2\alpha}\,|V^{\alpha\beta}_{\bar{m},\bar{m}+\bar{g}}|\,\delta(E_\alpha - E_\beta)\,. \qquad (28)$$

h means here the matrix element of H' between nearest sites and z the number of nearest sites. The frequency Ω_1 equals $\Omega_{\bar{m}\bar{n}} = \Omega_{\bar{m}-\bar{n}} = \Omega_{\bar{g}}$ where $\bar{g}$ is the difference between neighbouring sites, $\bar{m}-\bar{n}=\bar{g}$. D_{coh} derives from the coherent tunneling of the particles and is limited by the correlation-breaking frequency or attenuation frequency of the non-diagonal elements of the density matrix. The correlation

breaking is due to intrasite scattering by phonons and the tunneling happens without the assistance of phonons. In contrast to this is the incoherent diffusion, in which tunneling into the neighbouring site takes place through excitation by the phonon system and so D_{incoh} is determined by intersite scattering. Taking into account that the particle distribution in the intra-well levels is of the Boltzmann type, the diffusion coefficient can be written

$$D = \sum_s (D_c^s + D_h^s) e^{-\epsilon_s/kT} Z^{-1} \qquad (29)$$

$$Z = \sum_s e^{-\epsilon_s/kT} \qquad (30)$$

and this gives the familiar activation-type exponent at high temperatures, where the overbarrier diffusion is strongest.

Kagan and Klinger [18] developed further the previous method by more detailed calculations and by using a two-phonon coupling as an interaction between the particle and the phonons. Klinger [19] revised the theory making it more general and using as interaction a multi-phonon coupling. In the following both of these theories shall be rewieved parallel and we shall present a few results, some of which will later be used in this study.

Kagan and Klinger showed that the basic scattering mechanism limiting the coherent diffusion is due to dynamical destruction of the bands, which is caused by fluctuations of the relative shifts of energy levels between neighbouring wells owing to the interaction between the ion and the phonons. They showed too that at high temperatures and at practical concentration of impurities the overbarrier diffusion is dominating.

Kagan and Klinger [18] started from the same equation of motion for the density matrix as Kagan and Maksimov, where their Hamiltonian was $H = H_0 + H'$. Here H_0 is diagonal in the phonon states and H' is off-diagonal corresponding to the interaction with phonons. They obtained, after similar calculations, the same result for Ω_1, which corresponds to two-phonon intraband scattering. Kagan and Klinger have evaluated Ω_1 (after this called Ω_{ib}) approximately at high temperatures within the Debye model

$$\Omega_{ib} \simeq \left(\frac{kT}{\hbar\omega_D}\right)^2 \omega_D \left(\frac{\omega_D}{\omega_p}\right)^4. \qquad (31)$$

$\hbar\omega_p$ is the characteristic gap for the bands. This result will later be used in connection with the relaxation of the particle distribution among the bands (in fact the distribution within a single band).

The expressions for the coherent and noncoherent (hopping) diffusion coefficients become of the following forms

$$D_c^s = \frac{z\alpha^2\Delta_s^2}{3\hbar^2\Omega_{ib}^2} \approx \frac{z\alpha^2\mathcal{J}_s}{3\hbar^2\Omega_{ib}} \qquad (32)$$

being the approximate coherent part and

$$D_h^s = \frac{z\alpha^2}{3\hbar^2}\tau_s^2 e^{-2\phi^s(T)} \int_0^\infty dt \left(e^{\psi^s(t)} - 1\right). \qquad (33)$$

Here $\mathcal{J}_s$ equals the coherent bandwidth and

$$\psi^s(t) = \sum_\lambda \frac{2|W_\lambda(s)|^2(1-\cos(\bar{f}\cdot\bar{g}))\cos(\omega_\lambda t)}{\hbar^2 \sinh\left(\frac{\omega_\lambda}{2kT}\right)}, \qquad (34)$$

$$\phi^s(T) = \sum_\lambda |W_\lambda(s)|^2 (1 - \cos(\bar{f}\cdot\bar{g}))(1 + 2\bar{n}_\lambda) \qquad (35)$$

and

$$W_\lambda(s) = \sqrt{2M\omega_\lambda^3 N} \sum_j \left(\frac{\partial V(\bar{r},\bar{R})}{\partial \bar{R}_j}\Big|_{\bar{R}^\circ} \right)_{ss} \hat{e}_\lambda \left(e^{i\bar{f}\cdot\bar{R}_j} - 1 \right). \qquad (36)$$

Here ω_λ is a normal mode frequency with wavevector $\bar{f}$ and polarization $\hat{e}_\lambda$ having the equilibrium occupation $\bar{n}_\lambda$.

Kagan and Klinger approximated these equations in order to obtain numerical results for real physical systems and after summing the contributions from all overbarrier bands at high temperature they gave the result

$$D_o \simeq \frac{z\alpha^2}{\hbar}\sqrt{\frac{\hbar^3 kT^* \omega_p}{2m\, l_o^2\, \Delta E}}. \qquad (37)$$

l_o is the width of the barrier ($\approx\alpha$) and $\omega_p\cdot\hbar$ describes the typical underbarrier band gap; ΔE is the same for overbarrier bands. With this result in mind we shall estimate D_o numerically in section 3 c.

Finally we can mention the recent quantum approach of Gorham-Bergeron [35]. He applied the Kubo expression for D to the problem of motion of hydrogen atoms in metals. He used as interstitial atomic wave functions harmonic states obtaining for D

$$D = \frac{1}{m}\sqrt{\frac{\pi\hbar^2 kT}{2(E_b + \frac{1}{2}\hbar\omega\bar{b}^2)}}\, \exp\left\{ -\frac{1}{2kT}\left(E_b + \tfrac{1}{2}\hbar\omega\bar{b}^2\right) - \frac{\hbar\omega}{2kT\left(2\bar{b}^2 + \frac{E_b}{\hbar\omega}\right)} \right\}, \qquad (38)$$

where

$$\vec{b}^2 = b^2\left(\frac{m\omega}{2\hbar}\right) \tag{39}$$

b being the jump distance and E_b is the binding energy of the lattice deformation caused by the interstitial. $\frac{1}{4}\vec{b}^2\hbar\omega$ describes approximately the height of the potential barrier U_o.

In the following chapters we will represent, in more detail, an application of some of the preceding quantum theories to an existing and experimentally important diffusion problem; lithium in germanium and silicon.

Section a. in chapter 2 deals with the band structure of an interstitial in the lattice and shows how to calculate it when the interaction potential is known. In section b. the diffusion coefficient is calculated using Boltzmann's transport equation and the respective relaxation time is taken from Kagan and Klinger's theory just rewieved. Chapter 3 section a. is devoted to study the suitable potential model conforming to experimental activation energies. In the next section b. the band structures are calculated in detail and in section c. are the final expressions for D. The resulting band structures are shown in appendices F and G and appendix H shows the isotopic dependences of E_o and $\Delta\epsilon$. Chapter 4 discusses the results obtained and compares them with experimental values shown in table 3. in section 3 c.

2 DIFFUSION IN NARROW BANDS

a. Band model for interstitials

When an interstitial atom or ion moves in a perfect periodic crystal it experiences the lattice as periodic even in the case when it distorts the lattice around it over a large volume. By Bloch's theorem the particle behaves according to

$$\psi_{\bar{k}}(\bar{r}) = e^{i\bar{k}\cdot\bar{r}}\, u_{\bar{k}}(\bar{r}), \tag{40}$$

where $u_{\bar{k}}(\bar{r})$ is periodic in the lattice. Fluctuations of lattice atoms owing to thermal excitations can be handled in this model as perturbations although larger than in the case of electrons.

Using the Born-von Karman boundary conditions we obtain the allowed k-values in reciprocal lattice

$$\bar{k} = \sum_i \frac{n_i}{N} \bar{b}_i \tag{41}$$

and for the density of k-values $\frac{V}{(2\pi)^3}$. Because there is spin-degeneracy due to high temperatures, the density of states in energy is twice that of the electrons e.g. in the case of free particles.

The strongly repulsive potential between interstitial and lattice atoms causes the bands to separate and they become extremely narrow. The narrowing is mostly due to the large masses of solute atoms compared with electrons ($m \sim 10^3 \ldots 10^5 m_e$). The widths of the bands can easily be evaluated to be

$$\Delta\epsilon \simeq \frac{2\hbar^2\pi^2}{m_n^* a_0^2} \tag{42}$$

by supposing the bands to have a simple free-particle-like (see [11]) dispersion

$$\mathcal{E}_n(\bar{k}) = \mathcal{E}_n^{\circ} + \frac{\hbar^2 k^2}{2 m_n^*}. \qquad (43)$$

n is the band index and m_n^* is the effective mass in band n.

The width of a band tells us the size of the overlap of the interstitial wavefunctions between neighbouring interstitial sites. Since the velocity of a Bloch particle in a band is determined by the relation

$$\bar{v}_n(\bar{k}) = \frac{1}{\hbar} \nabla_{\bar{k}} \mathcal{E}_n(\bar{k}), \qquad (44)$$

we can infer that in these bands the velocities are small, of the order $2\pi\hbar/ma_o$. As long as there exists any overlap between the states of the neighbouring sites the particles will have finite velocities to move freely through the crystal. At high temperatures large fluctuations scatter the particles and their average free path becomes shorter than a lattice constant a_o.

We can use as the Bloch wave function a wave packet composed of all Bloch states in a given band

$$\psi_{\bar{k}}(\bar{r}) = \sum_{\bar{k}'} u_{\bar{k}'}(\bar{r})\, e^{i\bar{k}'\cdot\bar{r}} \qquad (45)$$

provided that $u_{\bar{k}}(\bar{r}) \approx 0$ when $|\bar{k}-\bar{k}'| > \Delta\bar{k}$. This wave packet is localized in $\bar{k}$-space around the value $\bar{k}$ and in spatial space we can use the uncertainty relation with the uncertainty in $\bar{k}$ of the order of the size of the Brillouin zone $2\pi/a_o$ (see García-Moliner [20])

$$\Delta x \, \Delta k \gtrsim \tfrac{1}{2} \quad \Rightarrow \quad \Delta x \gtrsim \frac{a_0}{4\pi}. \tag{46}$$

This certainly localizes the particle within one primitive cell.

The Schrödinger equation of a particle in a periodic repulsive potential can be solved by substituting for the wave function a set of plane waves with constant (in spatial variables) coefficients corresponding to the Fourier-expansion of the function

$$\psi(\bar{r}) = \sum_{\bar{q}} C_{\bar{q}} \, e^{i\bar{q}\cdot\bar{r}}. \tag{47}$$

This is the most straightforward (and most laborious) method to try and it has been used in this study as we are lacking methods to calculate band structures in repulsive potentials for massive particles.. We can expand the periodic lattice potential in a similar way (the explicit form of U(r) will be discussed later)

$$U(\bar{r}) = \sum_{\bar{K}} U_{\bar{K}} \, e^{i\bar{K}\cdot\bar{r}}, \tag{48}$$

$$U_{\bar{K}} = \frac{1}{v_c} \int_{cell} d\bar{r} \, e^{-i\bar{K}\cdot\bar{r}} \, U(\bar{r}). \tag{49}$$

Substitution and change of summation variables give (see app. B)

$$\det_{\bar{K}\bar{K}'} \left| U_{\bar{K}'-\bar{K}} + \left(\frac{\hbar^2}{2m} (\bar{k}-\bar{K})^2 + U_0 - \mathcal{E} \right) \delta_{\bar{K},\bar{K}'} \right| = 0. \tag{50}$$

From this relation we can solve $\mathcal{E} = \mathcal{E}(\bar{k})$ in the first Brillouin zone

by expanding the determinant. The function takes the form

$$\psi_{\bar{k}}(\bar{r}) = e^{i\bar{k}\cdot\bar{r}}\, u_{\bar{k}}(\bar{r}) \tag{51}$$

$$u_{\bar{k}}(\bar{r}) = \sum_{\bar{K}} c_{\bar{k}-\bar{K}}\, e^{-i\bar{K}\cdot\bar{r}} . \tag{52}$$

The resulting band structure contains in general some levels (at least one) below the potential barrier and the rest of the bands are at higher energies, see figure 4. below.

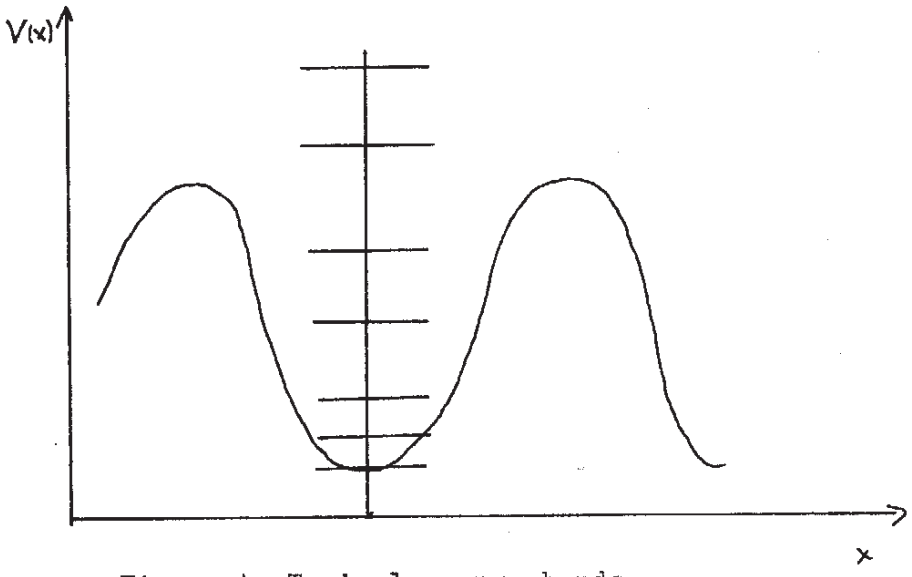

Figure 4. Typical energy bands

b. Calculation of the diffusion coefficient

The narrow bands of allowed particle energies are occupied by interstitial atoms and due to the high temperature they obey classical Boltzmann statistics. The degeneracy temperature is very low for massive particles (compared with electrons) ; e.g. for Li atoms $T_{deg} \simeq 10\,°K$ and even for H-atom it is less than 70 °K. The equilibrium occupation is the Boltzmann factor

$$f(\mathcal{E}) = \frac{e^{-\beta \mathcal{E}}}{Z(\beta)} . \tag{53}$$

The mechanism that brings the system to equilibrium after perturbations is particle-phonon intra-band scattering. Interband scattering gives a much smaller contribution to this due to the large number of phonons needed for the process (2-20) depending on the band structure. Interband transitions are possible because the transition between energy levels differing by ΔE can, by the uncertainty relation, take place within a time period $\Delta t \simeq \frac{\hbar}{\Delta E}$ ($\sim 10^{-15}$s for band gaps of order 0.4 eV) by absorbing or emitting the number of phonons necessary in succession (single phonon interaction times are shorter than 10^{-15}s, see [19]).

Klinger has calculated the relaxation time due to interband scattering and he gives (see Klinger [19])

$$\Omega_{IB} \simeq \Delta E \left(\frac{kT}{\Delta E}\right)^{\nu} \tag{54}$$

$$\tau_{IB} = \Omega_{IB}^{-1} , \tag{55}$$

where ΔE is a typical band gap and ν tells how many phonons are needed in the process

$$\nu = \frac{\Delta E}{\hbar \omega_{ph}} . \tag{56}$$

In the Debye model ($\omega_{ph} \approx \omega_D$ for most phonons) we can evaluate this and we have

$$\Omega_{iB} \approx 10^2 \ldots 10^6 \ \frac{1}{s} \qquad (\nu = 3 \ldots 20) \tag{57}$$

depending on the band gap. This compared with the intraband two-phonon inverse relaxation times (details later)

$$\Omega_{ib} \simeq 10^9 \ldots 10^{12} \ \frac{1}{s} \tag{58}$$

is an extremely small factor and we can neglect it totally in the calculation of the relaxation time

$$\frac{1}{\tau_{rel}} = \frac{1}{\tau_{iB}} + \frac{1}{\tau_{ib}} \simeq \frac{1}{\tau_{ib}} = \Omega_{ib} . \tag{59}$$

Kagan and Klinger [18] and Klinger [19] have stated that at high temperatures the overbarrier noncoherent diffusion (excitation of phonons) is dominating and we can neglect the underbarrier contribution. With this in mind we can calculate the mobility μ for interstitials in the relaxation time approximation assuming that the dominating mechanism for relaxation is a two-phonon intraband intra-site scattering as Klinger et al. have calculated.

We have, in appendix C, calculated the mobility by means of the Boltzmann transport equation under the action of a small external field on the charged interstitial ions. The Nernst-Einstein relation

$$\mu = M \beta z e D \tag{60}$$

has been used to connect μ and D. Here M is an empirical coefficient which depends on solute-solvent pairs. In the case of Li in Ge and Si, M has been observed experimentally to be equal to 1.0 (see Shaw [21]). We obtain

$$D = \frac{\int_{B.Z.}^{\epsilon \geq \epsilon_0} d\bar{k}\, v_{\bar{k}}^2 \cos^2\theta\ \tau(\bar{k})\, f^0(\bar{k})}{\int_{B.Z.}^{\epsilon \geq 0} d\bar{k}\, f^0(\bar{k})} . \tag{61}$$

The denominator acts here as a partition function and normalizes the numerator.

To transform D to a form suitable for numerical calculations we need to do some approximations. First we must take $f^0(\bar{k})$ outside the integral sign because the variation of $f^0(\bar{k})$ in extremely narrow bands is vanishingly small and we get

$$D \simeq \frac{\sum_{j=n}^{\infty} e^{-\beta \mathcal{E}_j} \int_{B.Z.}^{band\ j} d\bar{k}\, v_{j\bar{k}}^2 \cos^2\theta\ \tau_j(\bar{k})}{\sum_{j=1}^{\infty} e^{-\beta \mathcal{E}_j} \int_{B.Z.}^{band\ j} d\bar{k}} , \tag{62}$$

where $\mathcal{E}_j$ means the lower edge of band j. The index n means naturally

the first band which exceeds the potential barrier. Next we shall approximate the Brillouin zone (the first one) with a sphere of the same volume v_B without making any crucial error. As can easily be seen the terms $j \geq n+1$ in the numerator are small compared with the dominating $j = n$ term due, of course, to the exponential functions in front of the integrals. This allows us to neglect all other terms provided that the difference between $\mathcal{E}_{n+1}$ and $\mathcal{E}_n$ is considerably more than kT.

With these approximations D becomes

$$D \simeq \frac{\sum_n^m e^{-\beta \mathcal{E}_j} \int_{v_B}^{\text{band}\,j} d\bar{k}\, v_{j\bar{k}}^2 \cos^2\theta\, \tau_j(\bar{k})}{v_B \sum_1^\infty e^{-\beta \mathcal{E}_j}}, \qquad \mathcal{E}_m - \mathcal{E}_n \lesssim kT. \tag{63}$$

Now we can use the relaxation time calculated by Kagan and Klinger [18] and Klinger [19], [23], which is based on two-phonon intraband scattering

$$\Omega_{ib} \simeq \left(\frac{kT}{\hbar\omega_D}\right)^2 \omega_D \left(\frac{\omega_D}{\omega_p}\right)^4, \tag{64}$$

where $\hbar\omega_p$ represents the typical (dominating) bandgap. Because Ω_{ib} is band-independent and does not have any $\bar{k}$-dependence we can take it in front of the summation

$$D \simeq \frac{\sum_n^m e^{-\beta \mathcal{E}_j} \int_{v_B} d\bar{k}\, v_{j\bar{k}}^2 \cos^2\theta}{\Omega_{ib}\, v_B \sum_{j=1}^\infty e^{-\beta \mathcal{E}_j}}. \tag{65}$$

This expression for D we can use in numerical calculations in the

next chapter after we have obtained the band structures.

The temperature dependence of D is primarily due to the exponential functions from two sources as can easily be seen; the term $e^{-\beta\varepsilon_n}$ in the numerator and $e^{-\beta\varepsilon_1}$ in the denominator giving

$$D \propto e^{-\beta(\varepsilon_n - \varepsilon_1)} \qquad (66)$$

and we can in most cases neglect the other terms. This is valid, of course, when assuming that the band gaps are relatively large ($\Delta E > kT$ and $kT \gg 0$). If two or more bands are very near each other, we can handle them as a single band (energy-averaged in some suitable way). The other bands act only at very high temperatures (often above T_m, the melting temperature) causing the otherwise straight-line behaviour in an Arrhenius-plot (logD vs. β) to bend. Clearly $\varepsilon_n - \varepsilon_1$ gives the classical activation energy, which in many cases is considerably larger than the height of the potential barrier.

The β-dependence of Ω_{ij} will be omitted in this study because the value given by Klinger et al. is only an estimation at high temperatures and it must be calculated at one single temperature T^* in the middle of the temperature range at hand. The same applies to D_0, which Kagan and Klinger gave and where we have the dependence $D_0 \propto \beta^{-1/2}$. This fact also strains other theories; we remember the theory of Nardelli and Reatto and the result of Gorham-Bergeron, where T has to be fixed (see also Flynn and Stoneham [16]).

3 APPLICATION OF THE THEORY

a. The potential model

The preceding theory is in this chapter used to calculate explicit numerical expressions for the diffusion coefficients of a lithium ion in germanium and silicon by first determining the interaction potential and calculating the energy band structures. The unknown potential parameters are fitted to achieve experimental activation energies after which D is available through application of the previous equations.

The lattice potential seen by the interstitial has the form

$$U(\bar{r}) = \sum_{\bar{R}_j, i} \mathcal{V}(\bar{r} - \bar{R}_j - \bar{d}_i) \,. \qquad (67)$$

$\mathcal{V}(r)$ is the direct ion lattice potential, which consists mainly of two parts; the dominating repulsive part coming from the overlap of tightly bound inner shell electrons and the screened Coulomb interaction between nuclei and the small attractive part coming from the polarization of host atoms surrounding the interstitial and possibly from other effects, e.g. van der Waals interaction. The distortion in the lattice structure caused by the interstitial around itself will in general bring a contribution to the migration energy but in the case of lithium we shall neglect this term because lithium has a small ionic radius (~0.60 Å) and is generally considered to have only a very small distorsive effect. All attractive terms will also be neglected in the following due to their smallness and because

their behaviour as a function of r is relatively flat (see [26]).

The lattice potential $U(\vec{r})$ was calculated with a computer using several models for the repulsive potential taking into account the contribution of several million surrounding atoms. The points in the primitive cell, where the potentials were calculated in double precision, are shown in appendix A. The tetragonal site T is located in the center of the conventional cell and has four nearest neighbours and the the hexagonal sites are located in the center of the six member ring composed of the lattice atoms. These sites are possibly the only points, where the lattice potential could reach its minimum (in case of repulsive potential) the other of them working as a saddlepoint, through which the diffusion occurs. In all of the calculations made it was revealed that the tetragonal site had a lower lattice potential, thus being the equilibrium point and the hexagonal point was the saddle point. Thus an atom residing at the T-site has four nearest equivalent T sites available to go to through the respective H site ($z = 4$).

The repulsive potential has acquired several forms in the theory of migration of atoms in semiconductors. A model called the Born-Mayer potential (see Weiser [24]) was earlier used in studying the atomic migration. It corresponds mainly to the repulsive action of core electrons and therefore has no diverging (r^{-1}) behaviour

$$V_{BM}(r) = A\, e^{-r/r_0} \qquad (68)$$

In this work calculations were made with V_{BM} but it had to be rejected due to its weakness, that is the potential barrier height

was far too low compared with experimental values together with the band model activation energy, which was calculated based on this model.

The second model employed in the calculations was the ordinary screened Coulomb potential (Shaw [26] and Nardelli and Reatto [9])

$$V_c(r) = A\, e^{-\lambda r} r^{-1}. \tag{69}$$

Here $1/\lambda$ is the screening length defined by the solute concentration and varies from 2 Å to 40 Å. It has been evaluated by Dingle [27] and Kennedy [30]. Dingle's suggestions varied from 40 Å in dilute solutions (calculated with his formulas) at about 1000 °K temperature, to 7 Å (Ge) and 4 Å (Si) at large concentrations (near the limit of solid solubility of Li). Kennedy proposed values between a_0 and 10 Å both for Ge and Si at practical concentrations.

The prefactor A has the form

$$A = \frac{Z_1 Z_2 e^2}{4\pi \epsilon_0 \epsilon} \tag{70}$$

ϵ being the dielectric constant Z_1 and Z_2 being determined by Pauling [29] and Swalin [28] from an empirical standpoint. Pauling introduced the concept of imperfect screening and a value of the screening coefficient 0.4 was found for electrons in valence orbitals and for deeper lying ion core electrons a value equal to 1.0. Because Ge and Si have four valence electrons forming the tetrahedral bonds this rule gives effective valence $Z_2 = 2.4$ for both atoms. Lithium exists in a singly ionized state and its value for

Z_1 will be 1.0 (if Li could be neutral in the lattice, Z_1 would be 0.6). The values of ϵ used in A are 16.0 for Ge and 11.8 for Si. The resulting band structure (only a few lowest bands are shown) for Li in Ge is shown in figure 5. as a function of λ. They are calculated with the methods presented in the next section.

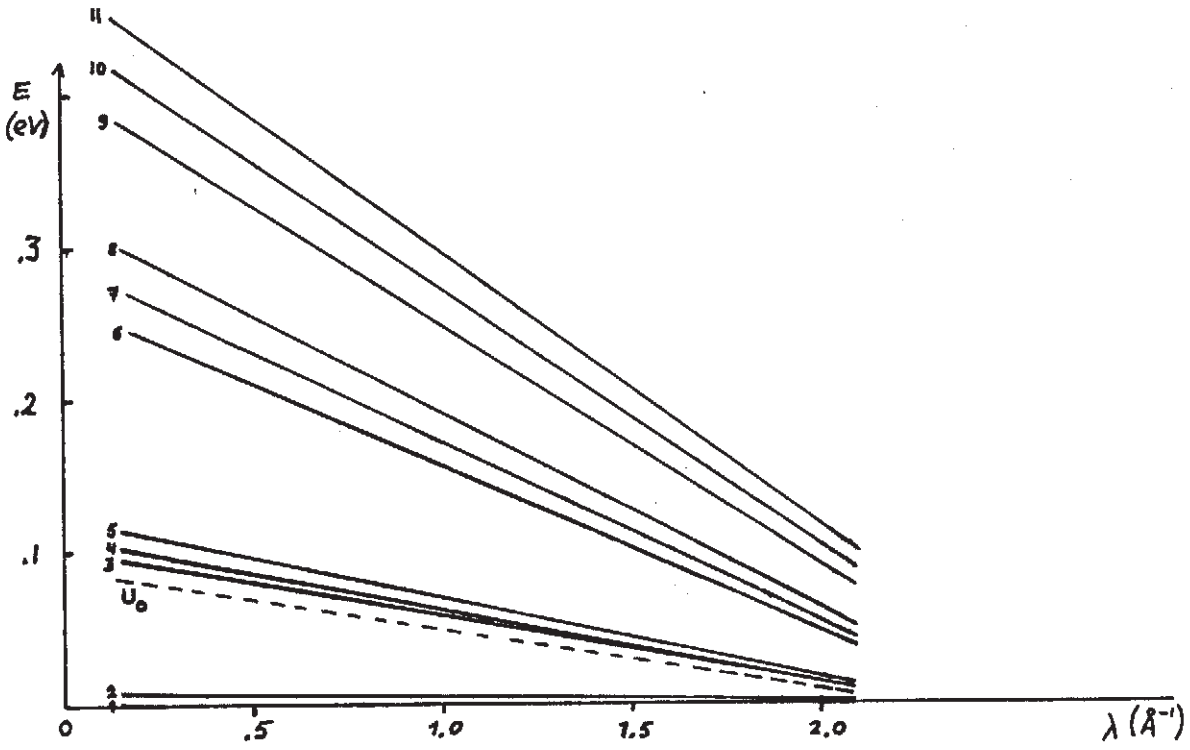

Figure 5. 11 lowest bands of Ge using V_c

The broken line represents height of the potential barrier calculated with the aid of lattice sums as described earlier. But the experimental value for U_o, the activation energy, is of order 0.5 eV so this model can not correspond to reality and it must be likewise rejected. In fact we can modify this potential to achieve satisfying results. The screened Coulomb potential corresponds mainly to the screened electrostatic interaction between positively charged nuclei without taking into account the repulsivity of ion

cores and weakening of screening at short distances ($r < r_I + r_L$, where r_I = ion core radius of Li $\approx$ 0.60 Å and r_L = r(Ge) $\approx$ 1.22 Å and for Si r(Si) $\approx$ 1.17 Å, see Weiser [24]). We can understand that the macroscopic dielectric constant ϵ must diminish as the interaction distance r becomes of microscopical order of length and it must approach its vacuum value 1.0 due to weakening of the screening. This transition from ϵ to 1 can be made in the spirit of screened interactions and we assume the following exponentially damping form for $\epsilon(r)^{-1}$

$$\frac{1}{\epsilon(r)} = \frac{1}{\epsilon}\left(1 + (\epsilon - 1)e^{-\alpha r}\right). \qquad (71)$$

This gives $\epsilon(r)^{-1} \approx 1/\epsilon$ at large distances and unity at very short r and this function can be substituted for $1/\epsilon$ in the expression for A

$$V(r) = \frac{Z_1 Z_2 e^2 e^{-\lambda r}(1 + (\epsilon - 1)e^{-\alpha r})}{4\pi\epsilon_0 \epsilon r}. \qquad (72)$$

This modification strengthens the potential at very short distances ($r \lesssim 1/\alpha$) taking at the same time into account the contribution from the repulsive cores. It also gives us two adjustable parameters. As can be seen from figure 5. the first overbarrier bands do not much change as a function of λ and this applies to the corrected model as well. The main variable is α and some typical graphs of bands calculated in this new model can be seen in appendix E as a function of λ and α. The potential barrier height has been shown in one of the figures as a broken line it being in the

gap between the third and fourth band in all cases calculated. Two more accurate graphs, used in the final determination of α , are shown in figures 6. and 7. There the potential barrier height has also been shown as a broken line.

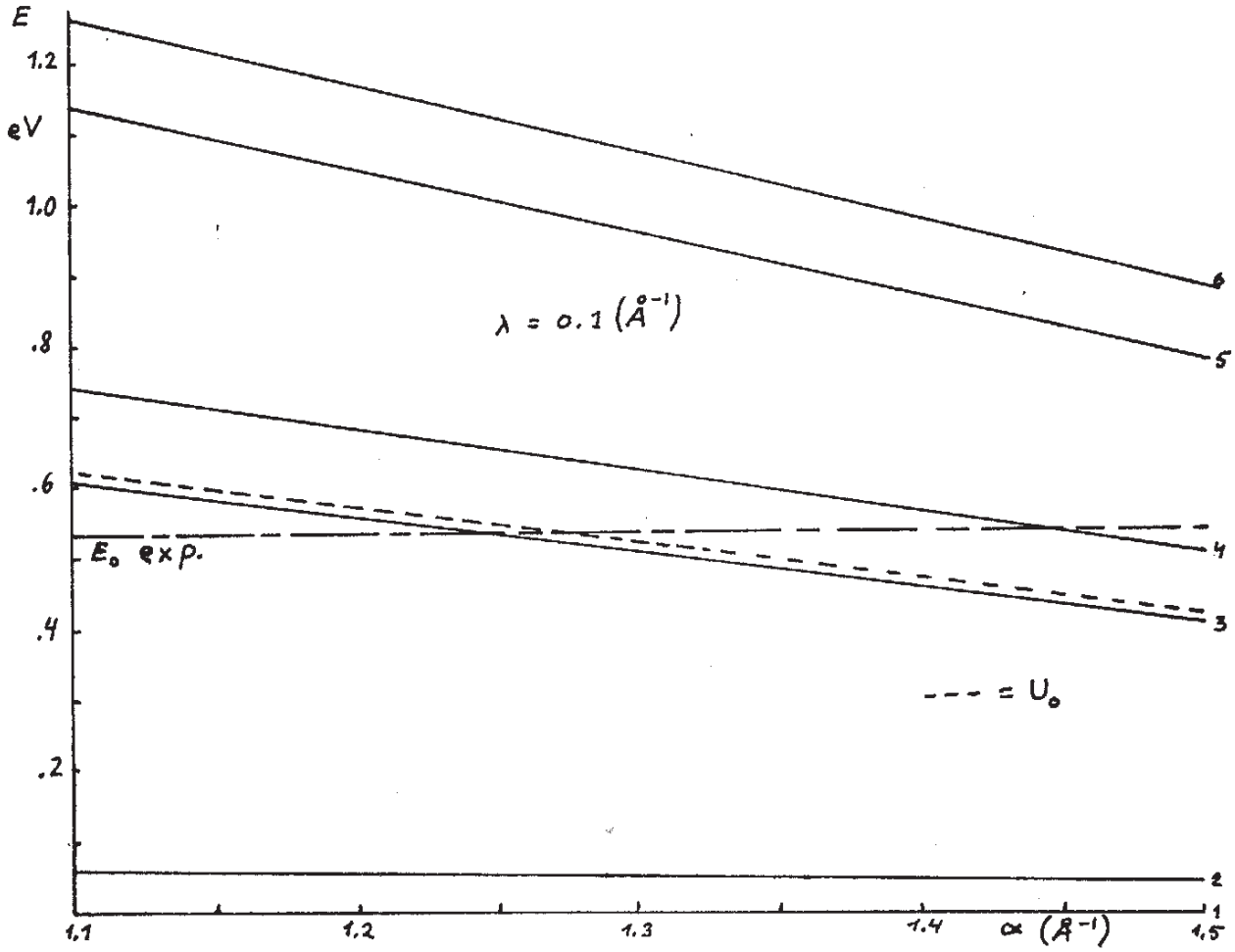

Figure 6. The band structure for the corrected potential (Ge) as a function of α.

Clearly this model gives realistic activation energies and we can now pick the proper values of λ and α. λ can be fixed by the previous arguments to have the value 0.1 $Å^{-1}$ for both Ge and Si corresponding to a screening length 10 Å being far from critical (see also appendix E). Thus the principal problem lies in choosing α.

It can be done by comparing the resulting activation energies with the experimental values (the energy is calculated from the difference between the first overbarrier and the lowest underbarrier bands), which are about 0.53 eV for Ge and 0.66 eV for Si. An extra criterion in choosing the ratio of the parameters α (Ge) and α(Si) was the fundamental ratio $a_0(Si)/a_0(Ge) \sim 0.96$ giving the length scale ratio and thus α (Si) was fixed by this ratio after the correct value of α (Ge) was obtained from the graphs. This method gave values of α for Ge and Si 1.45 and 1.39 respectively ($a_0(Si)/a_0(Ge) = \alpha(Si)/\alpha(Ge)$). The resulting value of α(Si) produced a value of activation energy, 0.64 eV, very close to the experimental value (see table 3. for all numerical values).

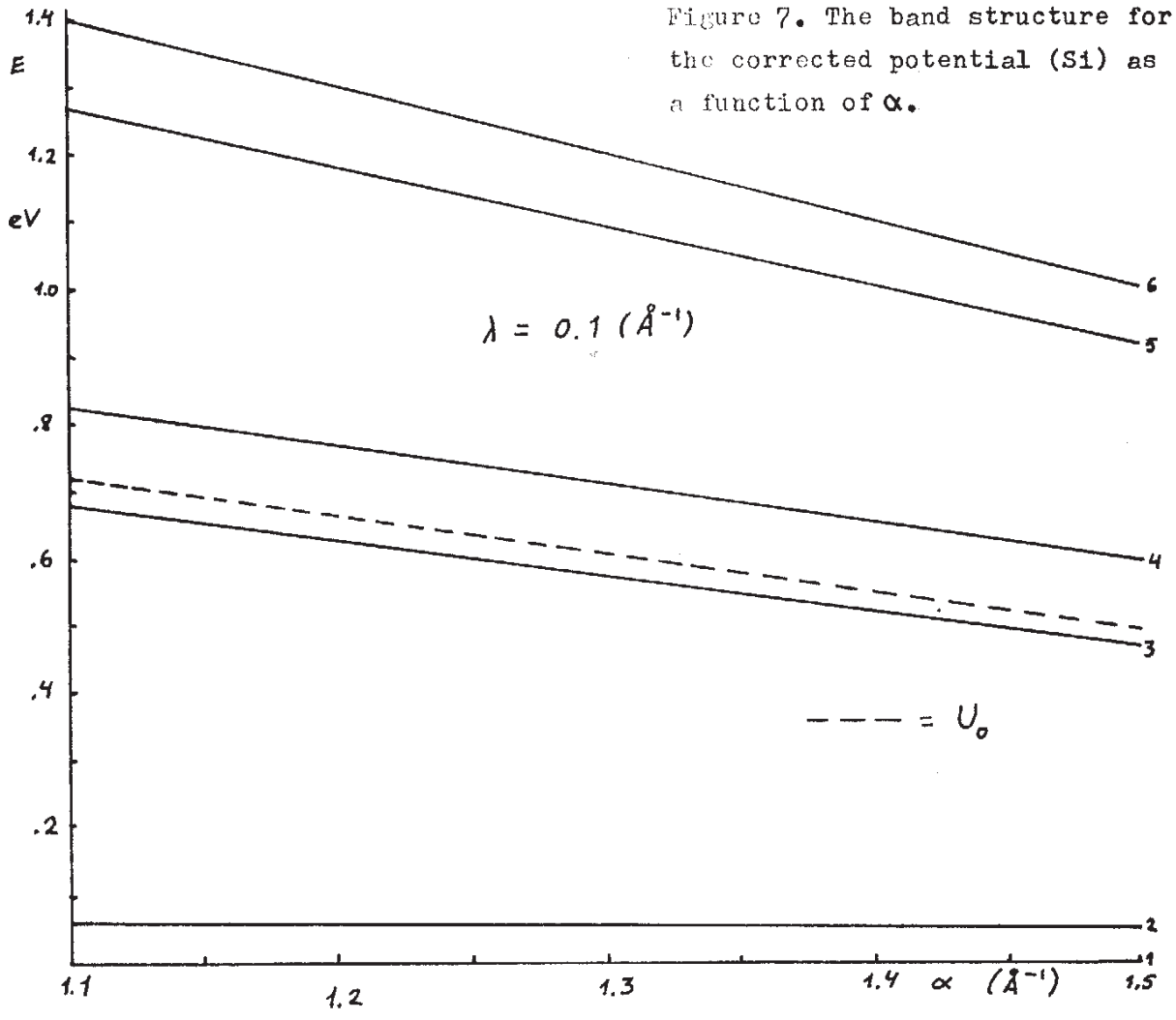

Figure 7. The band structure for the corrected potential (Si) as a function of α.

b. Calculation of band structures

As the potential model had been determined the band structure was calculated according to the principles shown in appendix B. In this section we will give some details of the method.

The complex determinant used was of 59 x 59 dimension defined by the 59 shortest reciprocal lattice vectors divided into six groups by their length (see table 1. below) .

Table 1. The 59 shortest reciprocal lattice vectors

length	0	$\frac{4\pi}{a_0}\frac{\sqrt{3}}{2}$	$\frac{4\pi}{a_0}$	$\frac{4\pi\sqrt{2}}{a_0}$	$\frac{4\pi\sqrt{11}}{a_0\ 2}$	$\frac{4\pi\sqrt{3}}{a_0}$
number of vectors	1	8	6	12	24	8

The reciprocal lattice vectors belong to the reciprocal lattice of diamond structure, which is body-centered cubic of cell side $4\pi/a_0$. The diamond lattice itself is face-centered cubic with the basis $\bar{d}_1 = (0,0,0)$ and $\bar{d}_2 = a_0/4(1,1,1)$, see appendix A. The existence of a basis causes the structure factor to differ from unity and in this case it is

$$S_{\bar{K}} = 1 + e^{i\bar{K}\cdot\bar{d}_2} = 1 + e^{\frac{i\pi}{2}(n_1+n_2+n_3)}, \qquad (73)$$

where the n_i are defined by the primitive vectors $\bar{b}_i$

$$\bar{b}_1 = \frac{2\pi}{a_0}(-\hat{i}+\hat{j}+\hat{k}),\quad \bar{b}_2 = \frac{2\pi}{a_0}(\hat{i}-\hat{j}+\hat{k}),\quad \bar{b}_3 = \frac{2\pi}{a_0}(\hat{i}+\hat{j}-\hat{k}), \tag{74}$$

$$\bar{K} = \sum_i n_i \bar{b}_i = \frac{4\pi}{a_0}(\nu_1 \hat{i} + \nu_2 \hat{j} + \nu_3 \hat{k}), \tag{75}$$

where $\nu_j = \frac{1}{2}(n_1 + n_2 + n_3) - n_j$,

$$\sum_1^3 \nu_j = \tfrac{1}{2}(n_1+n_2+n_3). \tag{76}$$

This gives for S_K

$$S_K = \begin{cases} 2, & \sum n_i = 2\sum \nu_i = \pm 4, \pm 8, \pm 12 \ldots. \\ 1+i, & = 1, 5, 9, 13 \ldots. \text{ (or } -3, -7, \ldots) \\ 1-i, & = 3, 7, 11, 15 \ldots \text{ (or } -1, -5, \ldots) \\ 0, & = \pm 2, \pm 6, \pm 10 \ldots. \end{cases} \tag{77}$$

Calculations were made with reciprocal lattice vectors less in number than 59 but satisfactory convergence of location of energy bands was achieved after 51 vectors. The preliminary calculations consisted of determining the band locations with sufficient accuracy with the $\bar{k}$-vector in the origin. As the final choice of the unknown parameters was performed, the dispersion relations could be calculated explicitly. The $\bar{k}$-space behaviour of $\xi(\bar{K})$ in the bands was examined in the first Brillouin zone for several symmetry directions (see figure 8.) starting from the origin and entering the corresponding symmetry points. Due to the large number of bands to be studied only three crucial symmetry points were employed in the

calculations (W, X and L). This was later justified by the extreme isotropies of the bands.

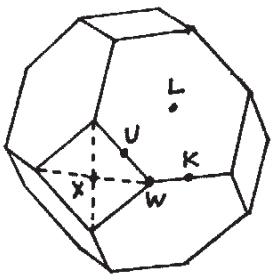

Figure 8. The first Brillouin zone and the symmetry points

To reduce the number of all symmetry directions belonging to respective points, two symmetries were used (see [25])

$$\mathcal{E}(-\bar{k}) = \mathcal{E}(\bar{k}) \quad , \quad \mathcal{E}(\bar{k} + \bar{K}) = \mathcal{E}(\bar{k}). \qquad (78)$$

The directions left are shown in table 2. below.

Table 2. (vectors shown in units $4\pi/a_0$) Symmetry directions

$W_1 - W_6$	$L_1 - L_4$	$X_1 - X_3$
$(\frac{1}{2}, \frac{1}{4}, 0)$	$(\frac{1}{4}, \frac{1}{4}, \frac{1}{4})$	$(\frac{1}{2}, 0, 0)$
$(\frac{1}{2}, -\frac{1}{4}, 0)$	$(\frac{1}{4}, -\frac{1}{4}, \frac{1}{4})$	$(0, \frac{1}{2}, 0)$
$(\frac{1}{2}, 0, \frac{1}{4})$	$(\frac{1}{4}, -\frac{1}{4}, -\frac{1}{4})$	$(0, 0, \frac{1}{2})$
$(\frac{1}{2}, 0, -\frac{1}{4})$	$(\frac{1}{4}, \frac{1}{4}, -\frac{1}{4})$	
$(\frac{1}{4}, 0, \frac{1}{2})$		
$(\frac{1}{4}, \frac{1}{2}, 0)$		

Naturally all calculations were based on finding the zeros of the determinant with various values for parameters and energy. The determinant behaved very violently around its zeros as a function of energy and this caused troubles in finding the exact points of vanishing as the parameters were varying. The value of the determinant

could change from 10^{42} to -10^{42} within a change of E of the order 10^{-3} eV and back within a bit larger (10^{-2} eV) interval behaving as a θ-function about most of the zeros.

To approach the exact zero of the determinant a method was used, where the supposed energy range was divided into parts by a simple halving method until the zero was within a sufficiently small interval. One restricting factor in choosing the method was the number of determinants necessary to calculate to obtain the next iterated value of the energy (e.g. derivatives). The number of extra determinants had to be limited due to the rather long processing time for the computer to expand one single determinant.

With these methods the behaviour of $\mathcal{E}$ in $\bar{k}$-space was determined and in appendix F we give the band energies for the six lowest bands and in appendix G we have the band structures for four lowest. It was not necessary to represent dispersion relations in all symmetry directions calculated due to the observed spherical symmetry.

c. Results for D

The numerical values for the diffusion coefficient will be calculated in this section by means of the transport theory, equation (65), and the result of Kagan and Klinger, equation (37). This will take place after we have obtained the dispersion relations of Li in Ge and Si in those bands, which participate in diffusion (essentially bands 1 and 4 for both cases).

The inverse transport time Ω_{ij}, from the theory of Kagan and Klinger, shall be used as the relaxation time. In its definition, equation (64), the typical band gap $\hbar\omega_p$ will be defined as the average of two essential gaps ($\omega_p \approx \sqrt{\omega_i \omega_j}$). In this work it will suffice to use ω_3 and ω_4 representing the typical gaps ($\omega_p \approx \sqrt{\omega_3 \omega_4}$). These will be obtained from the calculated (fitted) band models as well as the difference $\varepsilon_4 - \varepsilon_1$ needed in the exponent (see table 3. and appendices D and F).

For the temperature T^* we will use values in the middle of the experimental temperature range ($T^* = 900\ ^\bullet K$ for Ge and $T^* = 1100\ ^\bullet K$ for Si). This applies as well to the result for D_0 of Kagan and Klinger.

The bands calculated for lithium atoms in germanium and silicon (see appendix G) resemble the free-particle bands and the effective masses for all bands were calculated by fitting a parabola to the graphs

$$\varepsilon(\bar{k}) = A k^2. \qquad (79)$$

In all bands it was stated with sufficient accuracy (0.1%) that $m^* = m_{Li}$ both for Ge and Si.

Taking in the result of transport theory only the first overbarrier band into account and neglecting all others except the lowest in energy ($\mathcal{E}_1$) we obtain

$$D = D_0 \, e^{-\beta E_0}, \qquad E_0 = \mathcal{E}_n - \mathcal{E}_1 , \qquad n = 4 , \tag{80}$$

where

$$D_0 = \frac{\int_{v_B}^{\text{band 4}} d\bar{k}\, v_{\bar{k}}^2 \cos^2\theta}{\Omega_{ib}\, v_B} = \frac{\hbar^2 k_s^2}{5 m^2 \Omega_{ib}} . \tag{81}$$

Here k_s is the radius of the equal-volume sphere in $\bar{k}$-space. By using

$$v_B = \frac{(2\pi)^3}{v_c} = \frac{4\pi k_s^3}{3} \tag{82}$$

we have in terms of the volume of the primitive cell v_c

$$k_s = 2\pi \sqrt[3]{\frac{3}{4\pi v_c}} \tag{83}$$

and we have the final expression for D_0

$$D_0 = \frac{4\pi^2 \left(\frac{3}{4\pi v_c}\right)^{\frac{2}{3}} \hbar^2}{5 m^2 \Omega_{ib}} \tag{84}$$

$$\Omega_{ib} \propto \omega_D \left(\frac{\omega_D}{\omega_p}\right)^4 \left(\frac{kT^*}{\hbar\omega_D}\right)^2 . \tag{85}$$

The D_0 of Kagan and Klinger, equation (37), can be modified according to the present band model. From the band locations in

appendix F we observe that the band gaps are quite similar below and over the barrier. Thus we can set

$$\hbar \omega_p \simeq \Delta E. \tag{86}$$

l_0 can be approximated by α, the jump distance, which equals $a_0\sqrt{3}/4$ in the case of diamond structure, so finally

$$D_0 \simeq z \alpha \sqrt{\frac{kT^*}{2m}}. \tag{87}$$

Now we are in the position to give numerical estimates for D_0 and table 3. below represents these values calculated by means of the data given in appendix D. In table 3. there are also some experimental values and results from other theories.

The isotopic dependences of $\Delta\epsilon$, the width of band number 4, and the activation energy E_0 were also studied in germanium by varying the particle mass within limits +100%...-50%. Results of this calculation are shown in appendix H and we can see the fact (which is verified by an accurate numerical fitting) that the bandwidth behaves as (symmetry point W_6)

$$\Delta\epsilon(4) = \frac{A}{m}. \tag{88}$$

The activation energy obeys the law equally accurately

$$E_0 = \frac{B}{m} + C. \tag{89}$$

To study the isotopic dependence of D_0 in the transport theory, we

Table 3. Results for $D = D_0 e^{-\beta U_0}$

	D_0(Ge) cm^2/s	D_0(Si) cm^2/s		U_0(Ge) eV	U_0(Si) eV
this work	$3.7\ 10^{-3}$ transp. th. eq. (84)	$1.1\ 10^{-3}$ transp. th. eq. (84)	this work (band model fitted)	0.53 ($\mathcal{E}_4 - \mathcal{E}_1$)	0.64 ($\mathcal{E}_4 - \mathcal{E}_1$)
	$7.2\ 10^{-3}$ Kagan, Klinger eq. (87)	$7.6\ 10^{-3}$ Kagan, Klinger eq. (87)		-	-
exp. results	$1.3\ 10^{-3}$ [36]	$2.7\ 10^{-3}$ [38]	exp. results	0.46 [36]	0.62 [38]
	$2.5\ 10^{-3}$ [37]	$2.5\ 10^{-3}$ [40], [41]		0.51 [37]	0.66 [40], [41]
	$9.1\ 10^{-3}$ [38]	$2.2\ 10^{-3}$ [39]		0.56 [38]	0.70 [39]
	-	$3.3\ 10^{-3}$ [37]		-	0.65 [37]
	-	$4.4\ 10^{-3}$ [36]		-	0.78 [36]
other theories	$1.7\ 10^{-3}$ [24]	$1.6\ 10^{-3}$ [24]	other theories	0.57 [24]	0.52 [24]
	$3.6\ 10^{-3}$ [9]	$2.6\ 10^{-3}$ [9]		-	-
	$0.44\ 10^{-3}$ [10]	$0.94\ 10^{-3}$ [10]		-	-

must take into account the m-dependence of Ω_{ik} (see [19])

$$\Omega_{ik} \propto m^{-\frac{1}{2}} \qquad (90)$$

giving for D_o

$$D_o \propto m^{-\frac{3}{2}}. \tag{91}$$

The mass dependence of the result of Kagan and Klinger, equation (87), has clearly the form

$$D_o \propto m^{-\frac{1}{2}}. \tag{92}$$

4. DISCUSSION

Now we are able to compare the results of our calculations with the experimental results and other theoretical calculations.

As we can see in appendix D all calculated results for D_0, both in transport theory and Kagan and Klinger's theory are of the same order of magnitude as the experimental values of D_0, which are rather diffuse and lack precise measurements over large temperature intervals. Other theoretical results are just as diffuse and scattered as can be seen in appendix D table 2. D_0 from transport theory is rather critical in the definition of ω_p and a relatively small change in it can shift D_0 by an order of magnitude.

The temperature dependence of Ω_{ib} is quite strong giving D_0 a dependence β^2, which has a too large impact on the total behaviour of D as a function of temperature (see appendix I). This anomaly was referred to in section 2.b. This shows clearly that the relaxation time must be calculated more precisely taking into account corrections from all phonon processes in addition to the two-phonon one.

The D_0:s of Kagan and Klinger agree well with the experimental values showing that their theory is valid at high temperatures although the weak dependence $D_0 \propto \beta^{\frac{1}{2}}$ is not exactly in accord with the experimental behaviour, which to a high degree of accuracy is a straight line in an Arrhenius-plot (see appendix I).

The isotopic behaviour of D_0 and E_0 are in the transport theory

$$D_0 \propto m^{-3/2}, \qquad (93)$$

$$E_o \propto \frac{A}{m} + B . \tag{94}$$

Let us for the sake of comparison recall some other theories : Flynn and Stoneham [16] have obtained in their theory the same behaviour for E_o in their oscillator model and for D_o the dependence $m^{\frac{1}{2}} e^{-3\sqrt{m}}$. Gorham-Bergeron [35] has achieved the same dependence for E_o also and for D_o he has the same result as Gosar [10] does

$$D_o \propto \frac{A}{m} . \tag{95}$$

Weiner [42] calculated hydrogen diffusion in metals also quantum mechanically in a harmonic oscillator approximation and he obtained

$$E_o \propto \frac{A}{\sqrt{m}} + B , \tag{96}$$

Klinger's theory gives the following (see ref. [19])

$$D_o \propto \frac{A}{m} , \tag{97}$$

$$E_o \propto \frac{B}{m} + C . \tag{98}$$

and finally the more general results of Kagan and Klinger [18] give

$$D_o \propto m^{-\frac{1}{2}} \text{ to } m^{-1} . \tag{99}$$

It seems evident that quantum theories in general give dependences $D_o \propto m^{\alpha}$ and $E_o \propto m^{\beta} + \gamma$, where $\alpha \simeq -\frac{1}{2} \ldots -1$ or stronger and $\beta = -1$.

This differs from the classical results, where D_0 is always exactly proportional to $m^{-\frac{1}{2}}$, E_0 having no m-dependence.

Experimentally the mass dependence is not solved because we are lacking precise experimental results and large fluctuations in this respect have been observed (see [43] and [44]).

The calculated bandwidths and gaps differ from those calculated by WKB-theory in the article of Kagan and Klinger [18]. For germanium we have (at W-point) $\Delta\epsilon \sim 5\cdot10^{-4}$ eV and the gap is $\Delta E \approx$ 0.05...0.4 eV (both for over- and underbarrier bands) compared with the results from the WKB-method

$$\Delta\epsilon \simeq \pi\sqrt{(\epsilon_n - U_0)\frac{\hbar^2}{2m\alpha^2}} \gtrsim 10^{-3}\ eV \qquad (100)$$

$$\Delta E \simeq \pi\sqrt{\frac{U_0\hbar^2}{2ma_0^2}} \gtrsim 10^{-3} - 10^{-2}\ eV\,. \qquad (101)$$

The widths are approximately of the same order but the gaps are much larger than predicted by the WKB-method.

The method employed in calculating the band structures in terms of plane wave expansions is very laborious and for future calculations some tight binding method should be developed to achieve results converging fast enough.

The relation $a_0(Si)/a_0(Ge) = \alpha(Si)/\alpha(Ge)$ used in fitting potential parameters succeeded satisfactorily when the Ge-parameters were first fitted and fixed and this gave an activation energy for Si very close to the experimental energies, indicating that the potential model is possibly of correct form. Of course it neglects the four bonds giving only a spherically symmetric pair

potential (the bonds are implicitly contained in the effective valence).

It seems that quantum theories are able to tell us more about the physics of diffusion in solids than classical ones but at the cost of more complicated calculations. There are however many questions for the quantum methods to answer, which classical theories can not treat, e.g. the concentration dependence of D and the motion of an interstitial atom in lattice dislocations and grain boundaries.

5. APPENDICES

Appendix A

Diamond structure and equilibrium sites

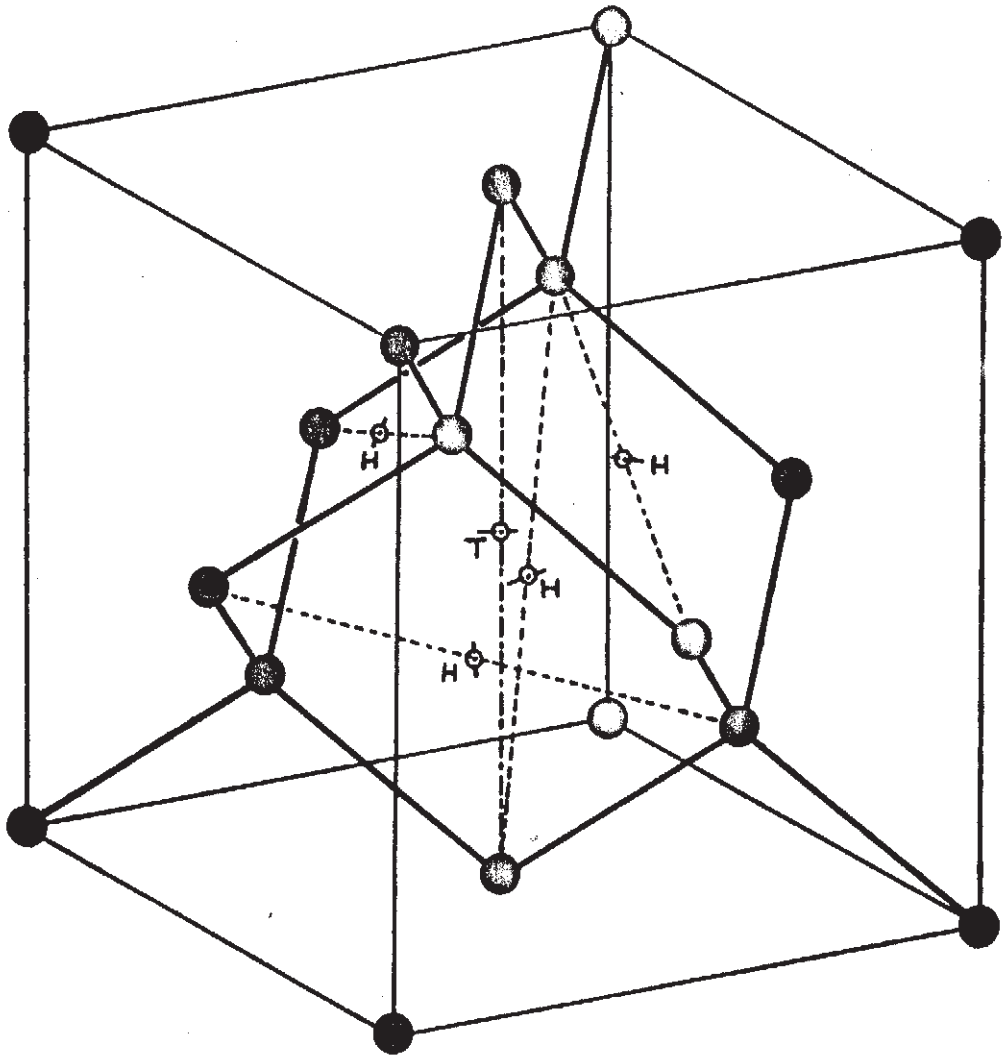

T = tetragonal site

H = hexagonal site

Appendix B

Solution of band structure

We choose the Fourier decomposition for the wave packet

$$\psi(\bar{r}) = \sum_{\bar{q}} C_{\bar{q}}\, e^{i\bar{q}\cdot\bar{r}}. \qquad (B\,1)$$

Here $C_{\bar{q}}$ are constant coefficients depending on the wave vector $\bar{q}$. The periodic lattice potential will be expanded similarly

$$U(\bar{r}) = \sum_{\bar{K}} U_{\bar{K}}\, e^{i\bar{K}\cdot\bar{r}}, \qquad (B\,2)$$

where

$$U_{\bar{K}} = \frac{1}{v_c}\int_{Cell} d\bar{r}\, e^{-i\bar{K}\cdot\bar{r}}\, U(\bar{r}) \qquad (B\,3)$$

and $\bar{K}$ belongs to the reciprocal lattice.

The kinetic energy term in the Schrödinger equation becomes

$$\sum_{\bar{q}} \frac{\hbar^2}{2m}\, q^2 C_q\, e^{i\bar{q}\cdot\bar{r}} \qquad (B\,4)$$

and the potential energy term is

$$U\psi = \sum_{\bar{K}} \sum_{\bar{q}} U_{\bar{K}}\, e^{i\bar{K}\cdot\bar{r}}\, C_{\bar{q}}\, e^{i\bar{q}\cdot\bar{r}} \qquad \bar{q}+\bar{K} \to \bar{q}' \to \bar{q}$$

$$= \sum_{\bar{K}} \sum_{\bar{q}} U_{\bar{K}}\, C_{\bar{q}-\bar{K}}\, e^{i\bar{q}\cdot\bar{r}}. \qquad (B\,5)$$

This gives us the Schrödinger equation

$$\sum_{\bar{q}} e^{i\bar{q}\cdot\bar{r}} \left\{ \left(\frac{\hbar^2 q^2}{2m} - \mathcal{E} \right) c_{\bar{q}} + \sum_{\bar{K}'} U_{\bar{K}'} c_{\bar{q}-\bar{K}'} \right\} = 0. \qquad (B\,6)$$

Coefficients of the plane waves must equal zero due to their independence and it follows

$$\left(\frac{\hbar^2 q^2}{2m} - \mathcal{E} \right) c_{\bar{q}} + \sum_{\bar{K}'} U_{\bar{K}'} c_{\bar{q}-\bar{K}'} = 0. \qquad (B\,7)$$

We will choose $\bar{q} = \bar{k} - \bar{K}$, so that $\bar{k}$ will always lie in the first Brillouin zone, and change the summation variable $\bar{K}' \to \bar{K}' - \bar{K}$ obtaining

$$\left(\frac{\hbar^2}{2m} (\bar{k} - \bar{K})^2 - \mathcal{E} \right) c_{\bar{k}-\bar{K}} + \sum_{\bar{K}'} U_{\bar{K}'-\bar{K}} c_{\bar{k}-\bar{K}'} = 0. \qquad (B\,8)$$

For this system of equations to have nonzero solutions the determinant of the coefficients of $C_{\bar{k}-\bar{K}}$ must be equal to zero (see [22])

$$\det_{\bar{K}\bar{K}'} \left| U_{\bar{K}'-\bar{K}} + \left(\frac{\hbar^2}{2m} (\bar{k} - \bar{K})^2 + U_0 - \mathcal{E} \right) \delta_{\bar{K}',\bar{K}} \right| = 0. \qquad (B\,9)$$
$$(\bar{K}' \neq \bar{K})$$

This solves us $\mathcal{E} = \mathcal{E}(\bar{k})$ in the bands provided that the infinite determinant is approximated by some finite one by taking a finite number of reciprocal lattice vectors symmetrically around the origin. In this way we obtain the dispersion relations in various directions in $\bar{k}$-space. Now $\bar{q}$ can only have values $\bar{k}$, $\bar{k}-\bar{K}_1$, $\bar{k}-\bar{K}_2$, etc, and therefore

$$\psi_{\bar{k}}(\bar{r}) = \sum_{\bar{K}} c_{\bar{k}-\bar{K}} e^{i(\bar{k}-\bar{K})\cdot\bar{r}} = e^{i\bar{k}\cdot\bar{r}} u_{\bar{k}}(\bar{r}). \qquad (B\,10)$$

We can calculate $U_{\bar{K}}$ in a general case as follows, the lattice potential being of the form

$$U(\bar{r}) = \sum_{\bar{R}_j, i} \mathcal{V}(\bar{r} - \bar{R}_j - \bar{d}_i). \tag{B 11}$$

Here $\mathcal{V}(r)$ is the interstitial ion-lattice atom potential and $\bar{d}_i$ describes the basis in the primitive cell. We recognize that the integration over the cell can be changed to an integration over the total crystal volume

$$U_{\bar{K}} = \frac{1}{\mathcal{V}_c} \int_{cell} d\bar{r}\, e^{-i\bar{K}\cdot\bar{r}} \sum_{R_j, i} \mathcal{V}(\bar{r} - \bar{R}_j - \bar{d}_i) = \frac{1}{\mathcal{V}_c} \int_{V} d\bar{r}\, e^{-i\bar{K}\cdot\bar{r}} \sum_{i} \mathcal{V}(\bar{r} - \bar{d}_i) \tag{B 12}$$

and the variable of integration can be changed as

$$U_{\bar{K}} = \frac{1}{\mathcal{V}_c} \sum_{j} e^{-i\bar{K}\cdot\bar{d}_j} \int_{V} d\bar{r}\, e^{-i\bar{K}\cdot\bar{r}} \mathcal{V}(\bar{r}) = \frac{S_{\bar{K}}\, \mathcal{V}_{\bar{K}}}{\mathcal{V}_c}. \tag{B 13}$$

$S_{\bar{K}}$ is the structure factor and $\mathcal{V}_{\bar{K}}$ is the Fourier transform of the interaction.

Finally we can calculate $\mathcal{V}_{\bar{K}}$ for the potential model chosen in section 3 a.

$$\mathcal{V}(r) = \frac{Z_1 Z_2 e^2}{4\pi\epsilon_0 \epsilon r} e^{-\lambda r} \left[1 + (\epsilon - 1) e^{-\alpha r}\right] \tag{B 14}$$

$$\mathcal{V}_{\bar{K}} = A \int d\bar{r}\, e^{\lambda r} \left(1 + (\epsilon - 1) e^{-\alpha r}\right) e^{-i\bar{K}\cdot\bar{r}} r^{-1}$$

$$= 4\pi A \left[\frac{1}{\lambda^2 + K^2} + \frac{\epsilon - 1}{(\lambda + \alpha)^2 + K^2}\right]. \tag{B 15}$$

For the diamond structure the structure factor is simply

$$S_{\bar{K}} = 1 + e^{i\bar{K}\cdot\bar{d}} \quad ; \quad \bar{d} = a_0 \left(\tfrac{1}{4}, \tfrac{1}{4}, \tfrac{1}{4}\right) \tag{B 16}$$

and we have finally

$$U_{\bar{K}'-\bar{K}} = \frac{4\pi A}{v_c}\left(1+e^{-i(\bar{K}'-\bar{K})\cdot\bar{d}}\right)\left[\frac{1}{\lambda^2+(\bar{K}'-\bar{K})^2}+\frac{\epsilon-1}{(\lambda+\alpha)^2+(\bar{K}-\bar{K}')^2}\right] \tag{B 17}$$

and

$$U_0 = \frac{8\pi A}{v_c}\left(\frac{1}{\lambda^2}+\frac{\epsilon-1}{(\lambda+\alpha)^2}\right). \tag{B 18}$$

Appendix C

Steady state solution of transport equation

We shall examine the influence of a weak external electric field on the distribution function of the interstitial ions and on the current, from which we will calculate the mobility μ. The basic assumption is the band model described earlier and knowledge of the band dispersion relations $\mathcal{E}_n = \mathcal{E}_n(\bar{k})$.

Boltzmann's equation for the distribution function is

$$\frac{d}{dt} f(\bar{k}) = \frac{\partial f}{\partial t}\Big|_{coll} + \frac{\partial f}{\partial t}\Big|_{field} . \qquad (C1)$$

The collision term becomes in the relaxation-time approximation

$$\frac{\partial f}{\partial t}\Big|_{coll.} = - \frac{f - f^o}{\tau} , \qquad (C2)$$

where τ is the time of relaxation of $f(\bar{k})$ and $f^o(\bar{k})$ is the equilibrium distribution

$$f^o(\bar{k}) = \frac{e^{-\beta \mathcal{E}(k)}}{Z(\beta)} \qquad (C3)$$

$\mathcal{E}(\bar{k})$ referring to all bands. The field term is

$$\frac{\partial f}{\partial t}\Big|_{field} = \dot{\bar{k}} \cdot \nabla_{\bar{k}} f = \frac{Ze\bar{E}}{\hbar} \cdot \nabla_{\bar{k}} f = \frac{Ze\bar{E}}{\hbar} \cdot \nabla_{\bar{k}} \mathcal{E}(\bar{k}) \left(\frac{\partial f}{\partial \mathcal{E}}\right), \qquad (C4)$$

Steady state solution of the transport equation is easily achieved

$$\frac{f - f^o}{\tau} = Ze\left(\bar{E} \cdot \frac{1}{\hbar} \nabla_{\bar{k}} \mathcal{E}(\bar{k})\right)\left(\frac{\partial f}{\partial \mathcal{E}}\right) = Ze\,(\bar{E} \cdot \bar{v}_{\bar{k}})\left(\frac{\partial f}{\partial \mathcal{E}}\right). \qquad (C5)$$

This has an approximate solution in the limit of a small external field

$$f \simeq f^{\circ} + \tau Ze(\bar{E}\cdot\bar{v}_k)\frac{\partial f^{\circ}}{\partial \epsilon}\,, \tag{C 6}$$

which becomes

$$f \simeq (1 - \tau\beta Ze(\bar{E}\cdot\bar{v}_k))\, f^{\circ}(\bar{k})\,. \tag{C 7}$$

The current density can be expressed in terms of f as follows

$$\bar{j} = -Ze\int_{B.Z.}^{\epsilon\geq\epsilon_0} d\bar{k}\,\bar{v}_k\,\frac{f(\bar{k})}{(2\pi)^3}\,. \tag{C 8}$$

Here the integration over the first Brillouin zone takes place only over those bands which participate in the current; that is bands exceeding the barrier, which will be denoted as $\epsilon\geq\epsilon_0$. So we have

$$\bar{j} = \beta Z^2 e^2 \int_{B.Z.}^{\epsilon\geq\epsilon_0} \frac{d\bar{k}}{(2\pi)^3}\,\bar{v}_k\,(\bar{v}_k\cdot\bar{E})\,\tau\, f^{\circ}(\bar{k}) \tag{C 9}$$

because the symmetric f°-term vanishes in the integration and the relaxation time has been considered to have some possible $\bar{k}$- or band-dependence.

On the other hand the density of particles (normalized as the current) can be determined by

$$n = \int_{B.Z.}^{\epsilon\geq 0} \frac{d\bar{k}}{(2\pi)^3}\, f(\bar{k}) = \int_{B.Z.}^{\epsilon\geq 0} \frac{d\bar{k}}{(2\pi)^3}\, f^{\circ}(\bar{k})\,. \tag{C 10}$$

The integration is here naturally over all bands and the small antisymmetric correction term vanishes in turn during the integration. Now we can define the mobility in the following manner

$$\bar{j} = \mu n Z e \bar{E} . \qquad (C\ 11)$$

We have assumed μ to be a scalar as always in cubic crystals (just as D is too). The preceding relation becomes

$$\beta Z e \int_{B.Z.}^{\epsilon \geq \epsilon_0} d\bar{k}\, \bar{v}_{\bar{k}} (\bar{v}_{\bar{k}} \cdot \bar{E}) \tau f^0(\bar{k}) = \mu \bar{E} \int_{B.Z.}^{\epsilon \geq 0} d\bar{k} f^0(\bar{k}) . \qquad (C\ 12)$$

Let us take the scalar product with $\bar{E}$ on both sides of the equation and choose the direction of the field in the $\bar{k}$-space along $\hat{k}_z$-axis.

$$\beta Z e \int^{\epsilon \geq \epsilon_0} d\bar{k}\, E^2 v_k^2 \cos^2\theta\, \tau f^0(k) = E^2 \mu \int^{\epsilon \geq 0} d\bar{k} f^0(\bar{k}) . \qquad (C\ 13)$$

This gives

$$\mu = \frac{\beta Z e \int^{\epsilon \geq \epsilon_0} d\bar{k}\, v_k^2 \cos^2\theta\, \tau f^0(\bar{k})}{\int^{\epsilon \geq 0} d\bar{k} f^0(\bar{k})} . \qquad (C\ 14)$$

Now we can assume the validity of the Nernst-Einstein relation

$$\mu = M \beta Z e D \qquad (C\ 15)$$

and we have for D

$$D = \frac{\int^{\epsilon \geq \epsilon_0} d\bar{k}\, v_k^2 \cos^2\theta\, \tau(k) f^0(\bar{k})}{M \int^{\epsilon \geq 0} d\bar{k} f^0(\bar{k})} . \qquad (C\ 16)$$

Appendix D

Table of important numerical values and results

entity	Ge	Si	ref. or expr.
a_o	5.66 Å	5.43 Å	[31]
v_c	45.33 $Å^3$	40.03 $Å^3$	$a_o^3/4$
ϵ	16.0	11.8	[9]
ϵ_o	$8.85416 \cdot 10^{-12}$ F/m		[32]
A	2.160 eVÅ	2.929 eVÅ	$Z_1 Z_2 e^2/(4\pi\epsilon_o\epsilon)$
Z_1	2.4	2.4	[9], [33]
Z_2(Li)	1.0	1.0	[9], [33]
m(Li)	$1.1526 \cdot 10^{-26}$ kg		[34]
	Final potential parameters fitted :		$V(r) = \frac{A e^{-\lambda r}}{r}(1-(\epsilon-1)e^{-\alpha r})$
λ	0.1 $Å^{-1}$	0.1 $Å^{-1}$	
α	1.45 $Å^{-1}$	1.39 $Å^{-1}$	see appendix E
	Lattice potential at sites T and H		
E_H	121.6035563 eV	186.4387375 eV	
E_T	121.1728025 eV	185.8995916 eV	see chapter 3 a.
ΔE	0.4307537719 eV	0.5391459428 eV	$\Delta E = E_H - E_T$
R_L	$40 \cdot a_o$	$40 \cdot a_o$	range of calculation, radius
z	4	4	number of nearest equivalent sites (see app. A)
T^*	900 °K	1100 °K	midpoint of high temp. range
ω_p	$7.2077\ 10^{14}$ 1/s	$8.7467\ 10^{14}$ 1/s	$\sqrt{\omega_3 \omega_4}$
ω_D	$4.7132\ 10^{13}$ 1/s	$8.1827\ 10^{13}$ 1/s	[31]
Ω_{ib}	$5.3861\ 10^{9}$ 1/s	$1.9415\ 10^{10}$ 1/s	$\omega_D \left(\frac{kT}{\hbar\omega_D}\right)^2 \left(\frac{\omega_D}{\omega_p}\right)^4$

The $\hbar\omega_i$ are the respective energies of bands with index i.

Band structure of Li in Ge as a function of potential parameters λ and α (showing some examples of calculated dependences).

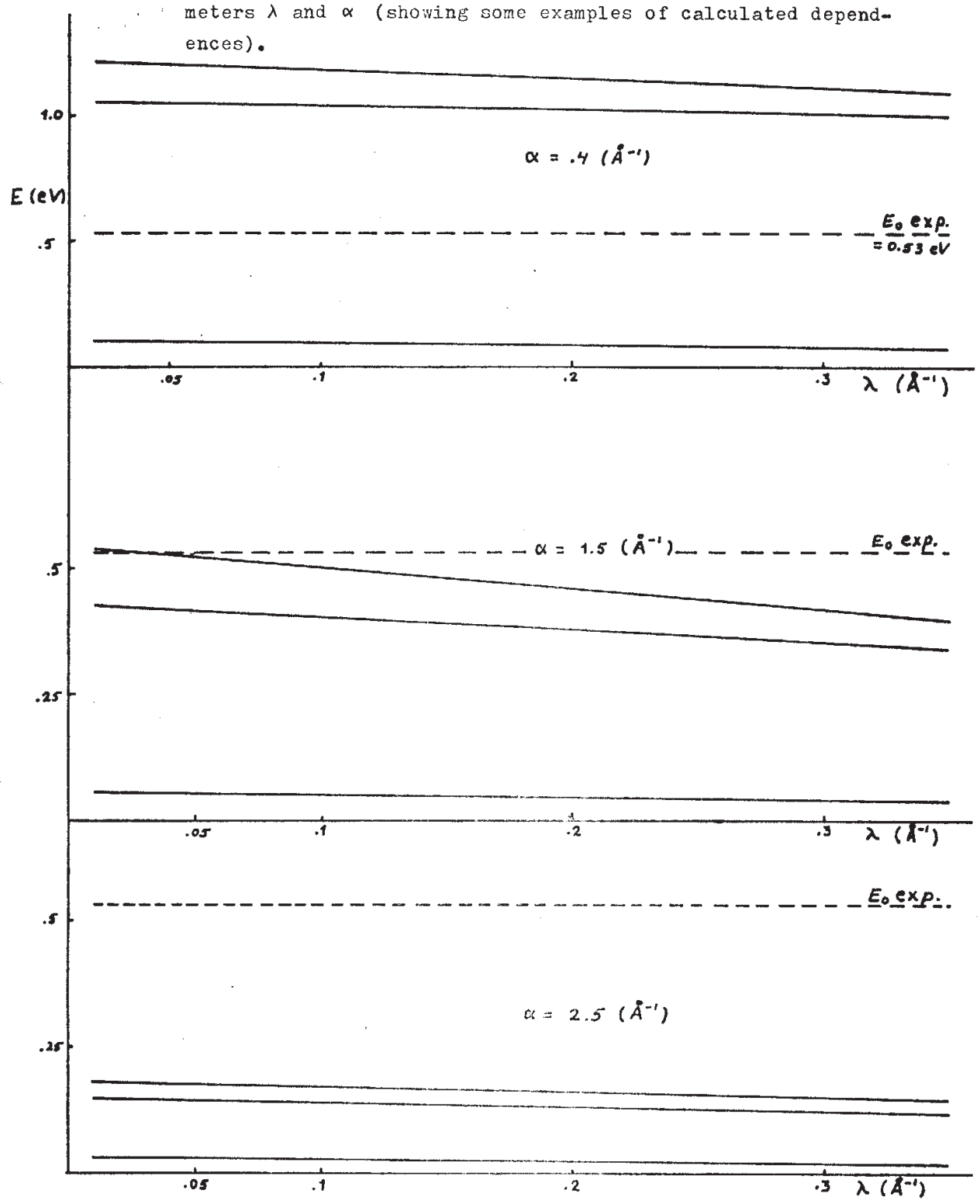

Band structure of Li in Ge as a function of λ with some values of the parameter α.

Appendix E cont'd.

Band structure of Li in Ge as a function of α with some values of the parameter λ.

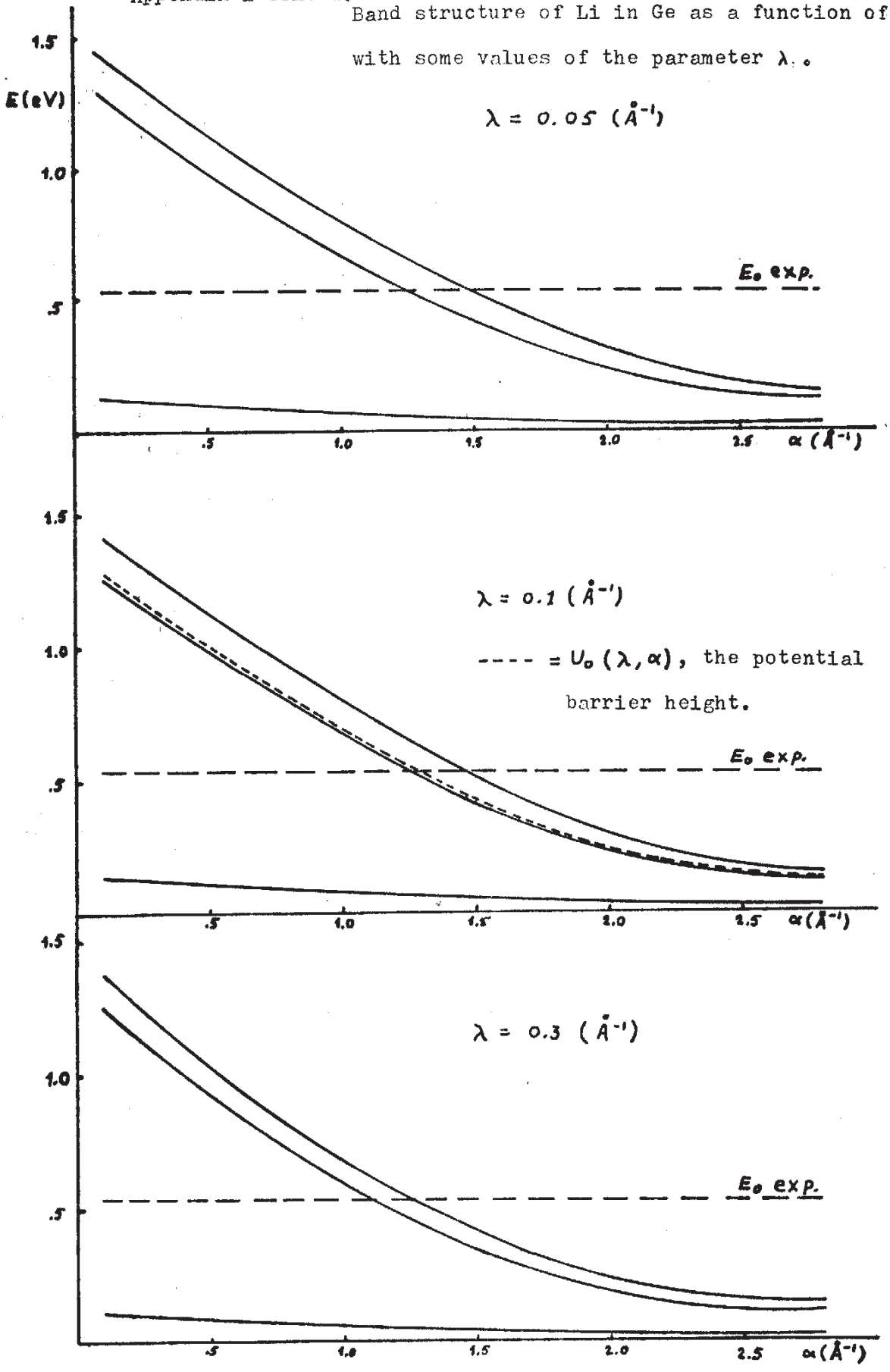

U_0 is situated in all graphs between the third and fourth bands.

Appendix F

Energy bands of Li in Ge and Si

U_o is the potential barrier height calculated as a difference in the lattice potential between the hexagonal and tetragonal sites.

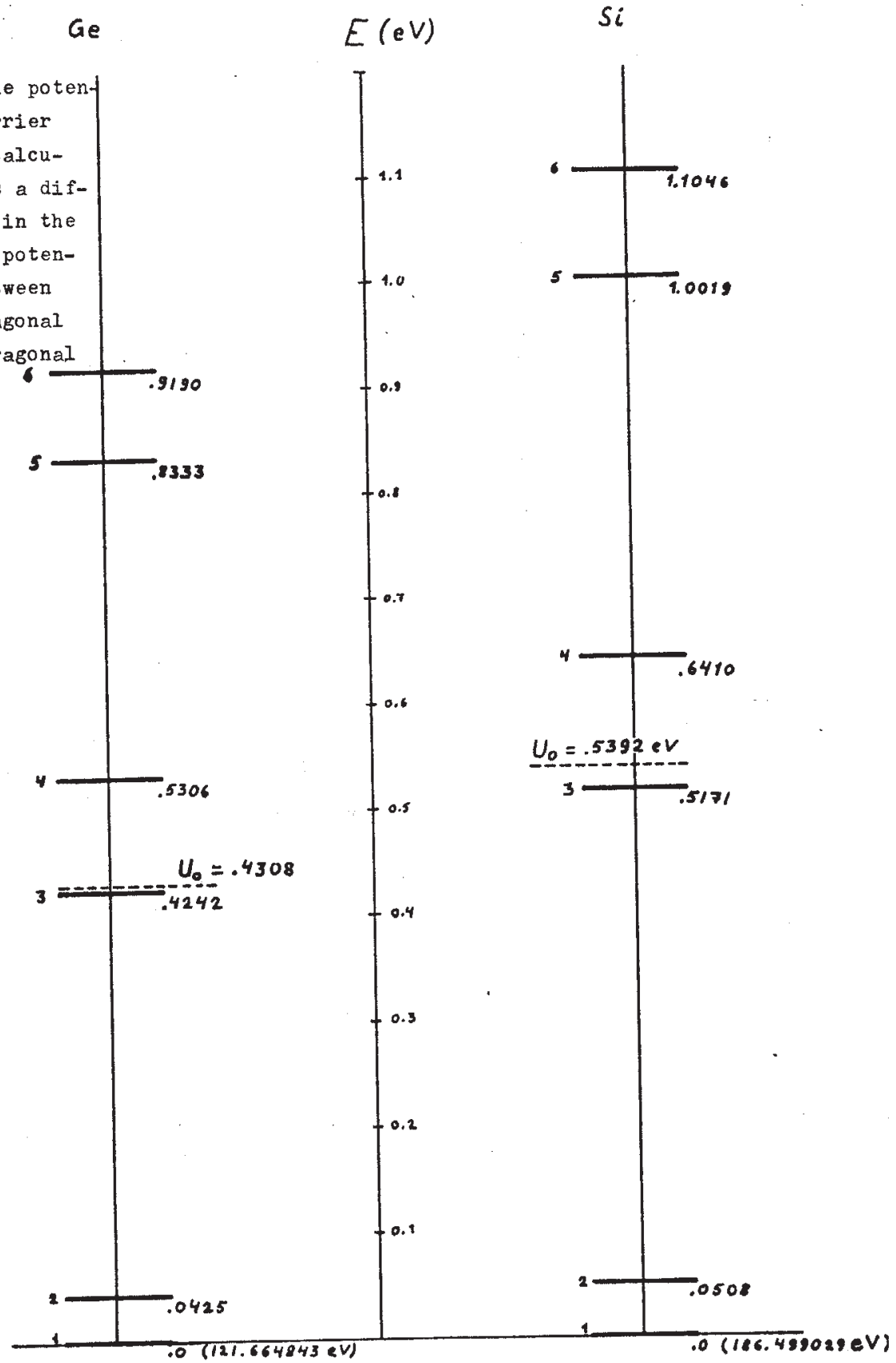

Appendix G

Band structures of Li in Ge and Si

Typical dispersion relations of Li in Ge. In all other symmetry directions in all bands the dispersions were the same as shown.

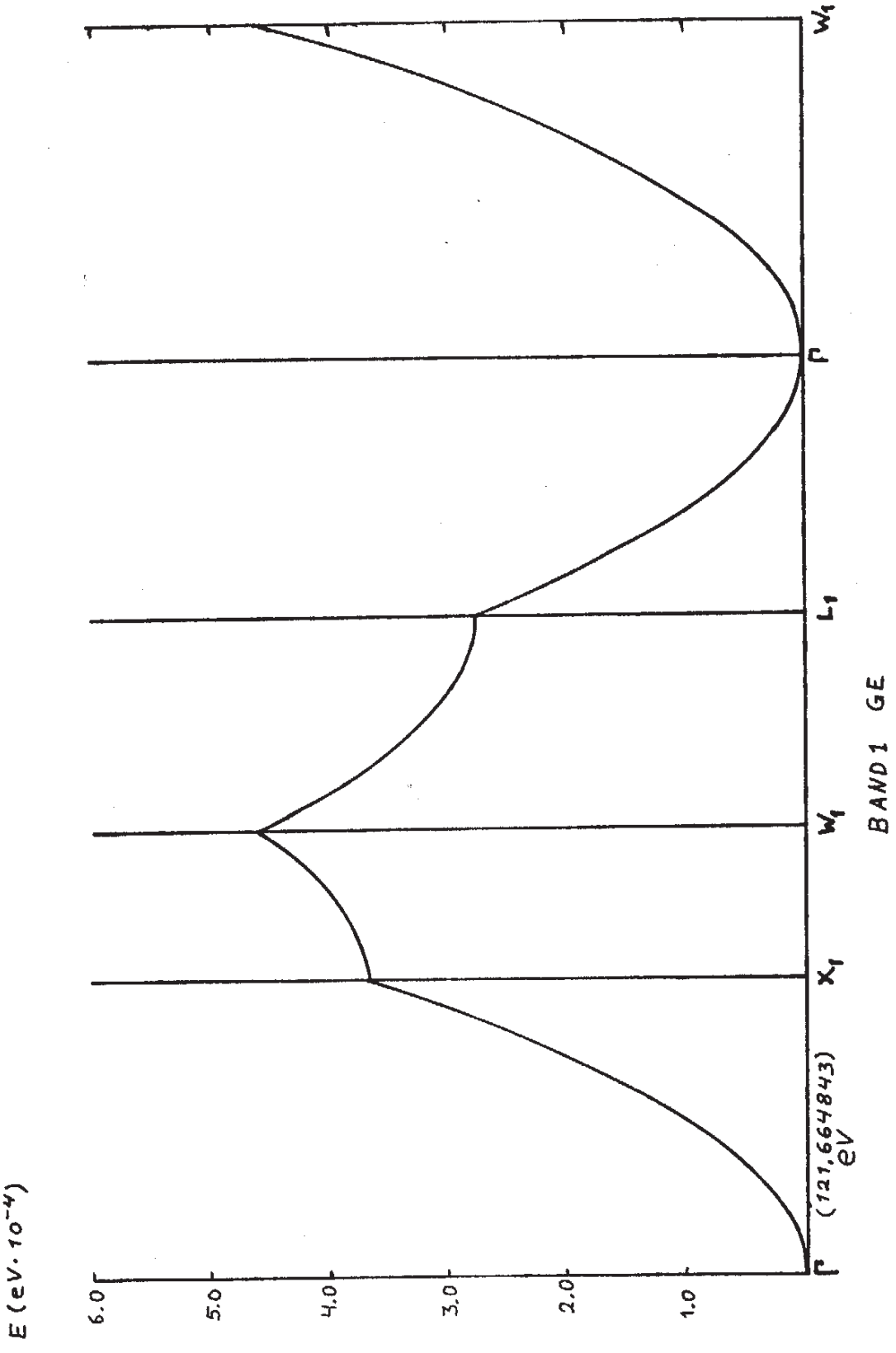

Appendix G cont'd

Typical dispersion relations of Li in Si. In all other symmetry directions in all bands the dispersions were the same as shown.

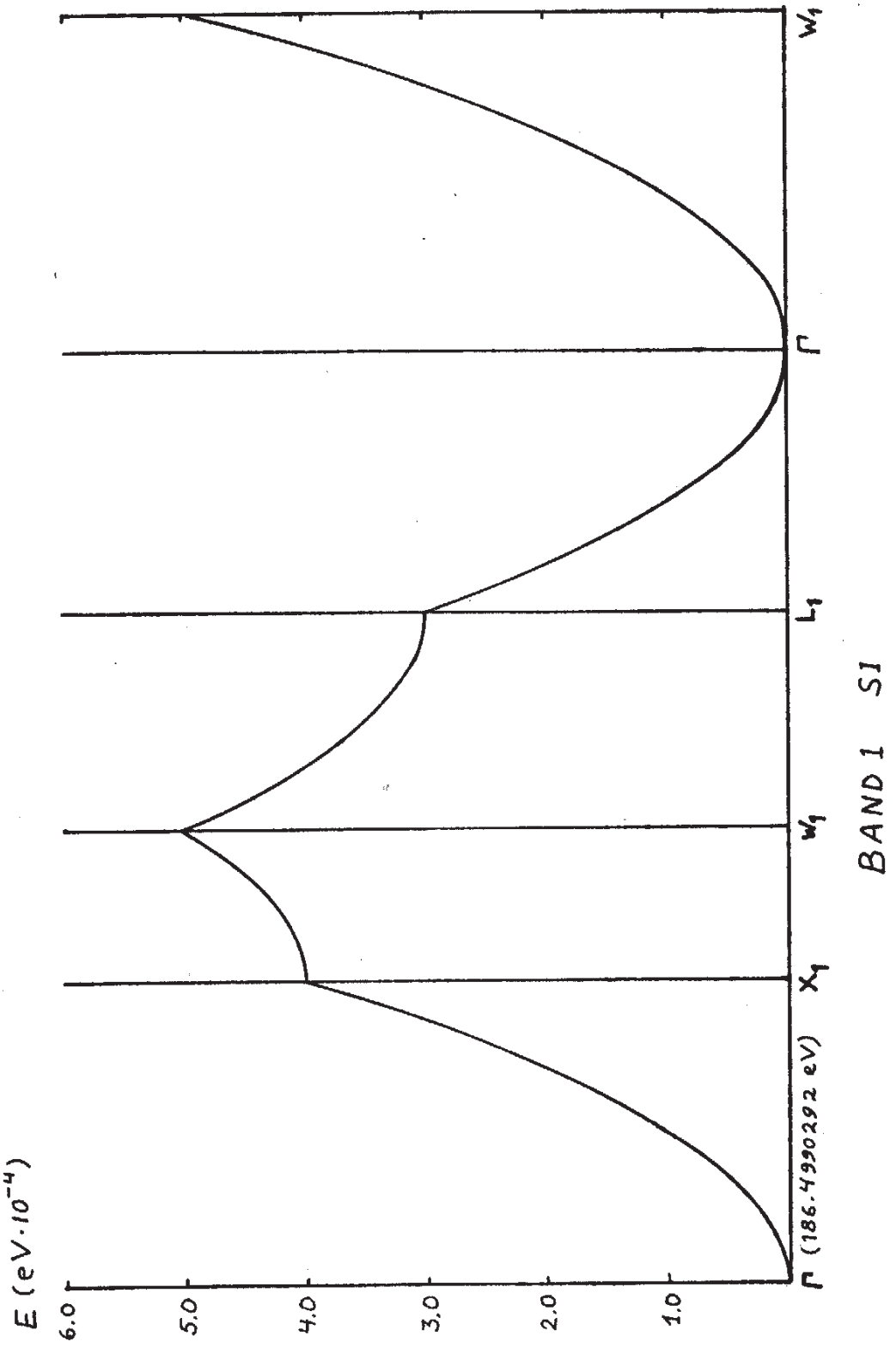

Appendix II

Isotopic dependences of E_0 and $\Delta\epsilon$ calculated from the band model (Ge band number 4)

Isotopic dependence of $\Delta\epsilon$.

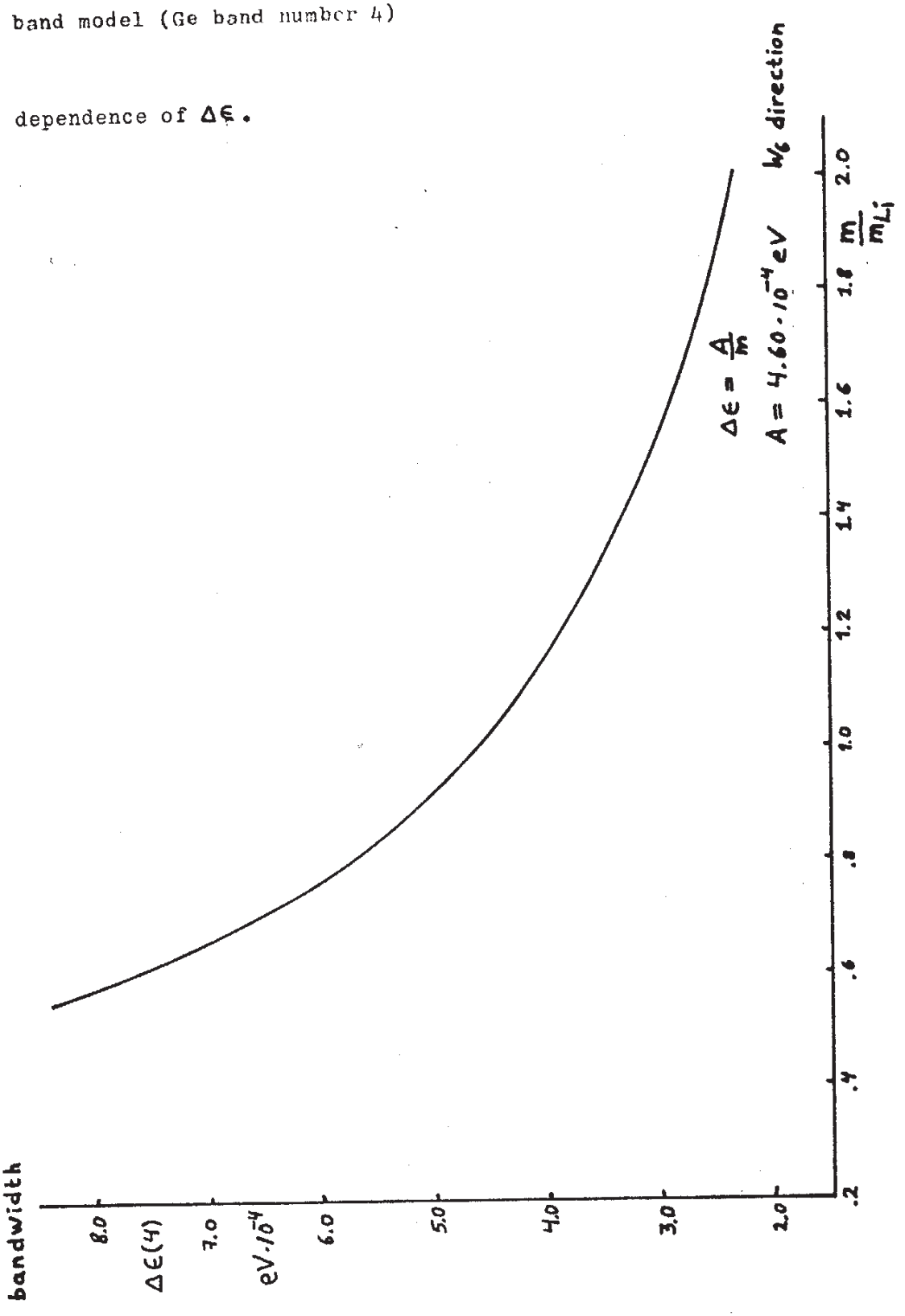

Appendix H cont'd

Isotopic dependence of E_o.

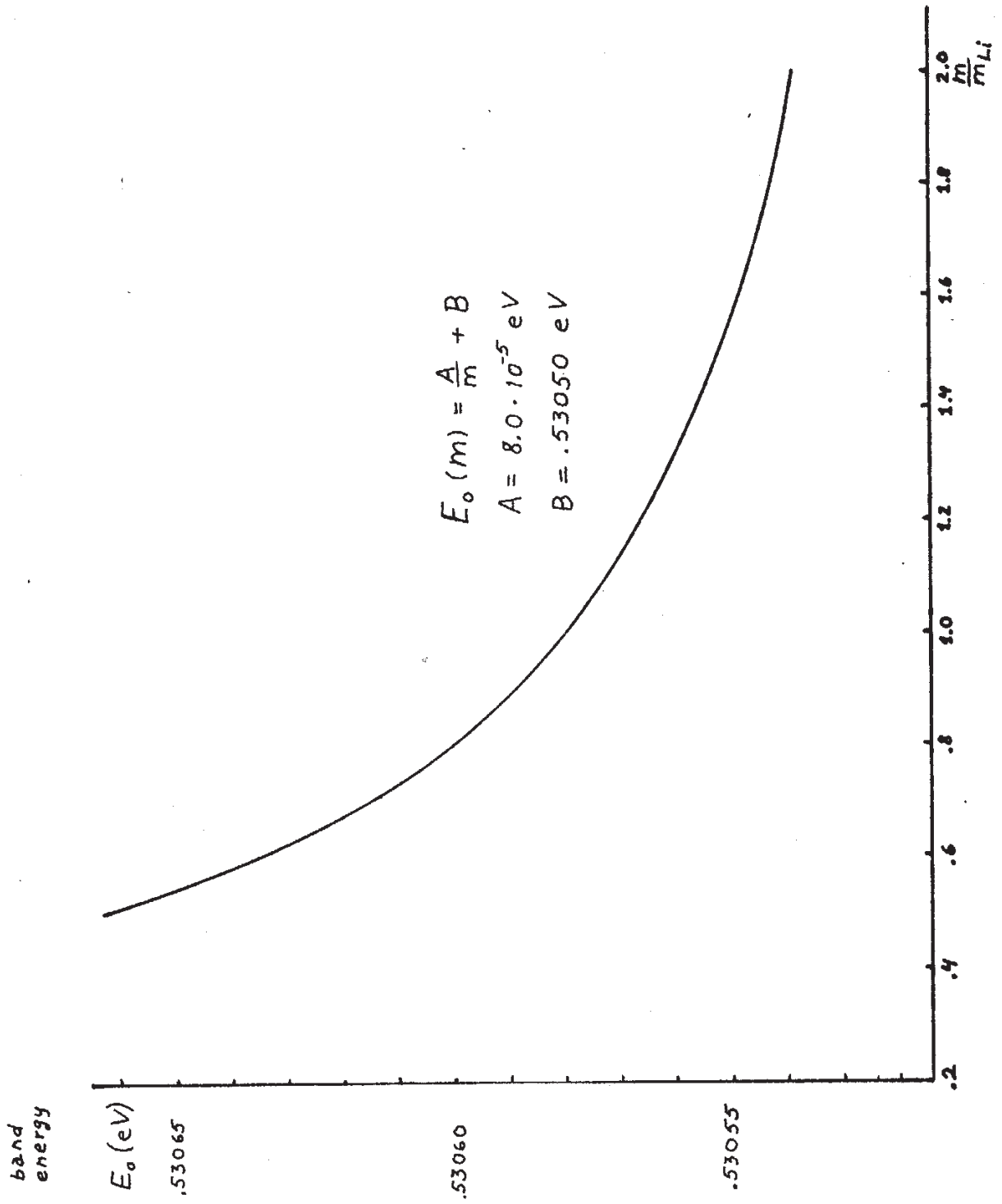

Appendix I

Temperature dependence of $D(\beta)$ in various cases in Ge

Graphs are calculated from the Ge band model and the experimental points are taken selectively from [36], [37] and [38].

$$D = D_0 \beta^n e^{-\beta U_0}$$

$D_0 \neq D_0(\beta)$

$U_0 \approx 0.53\ eV$

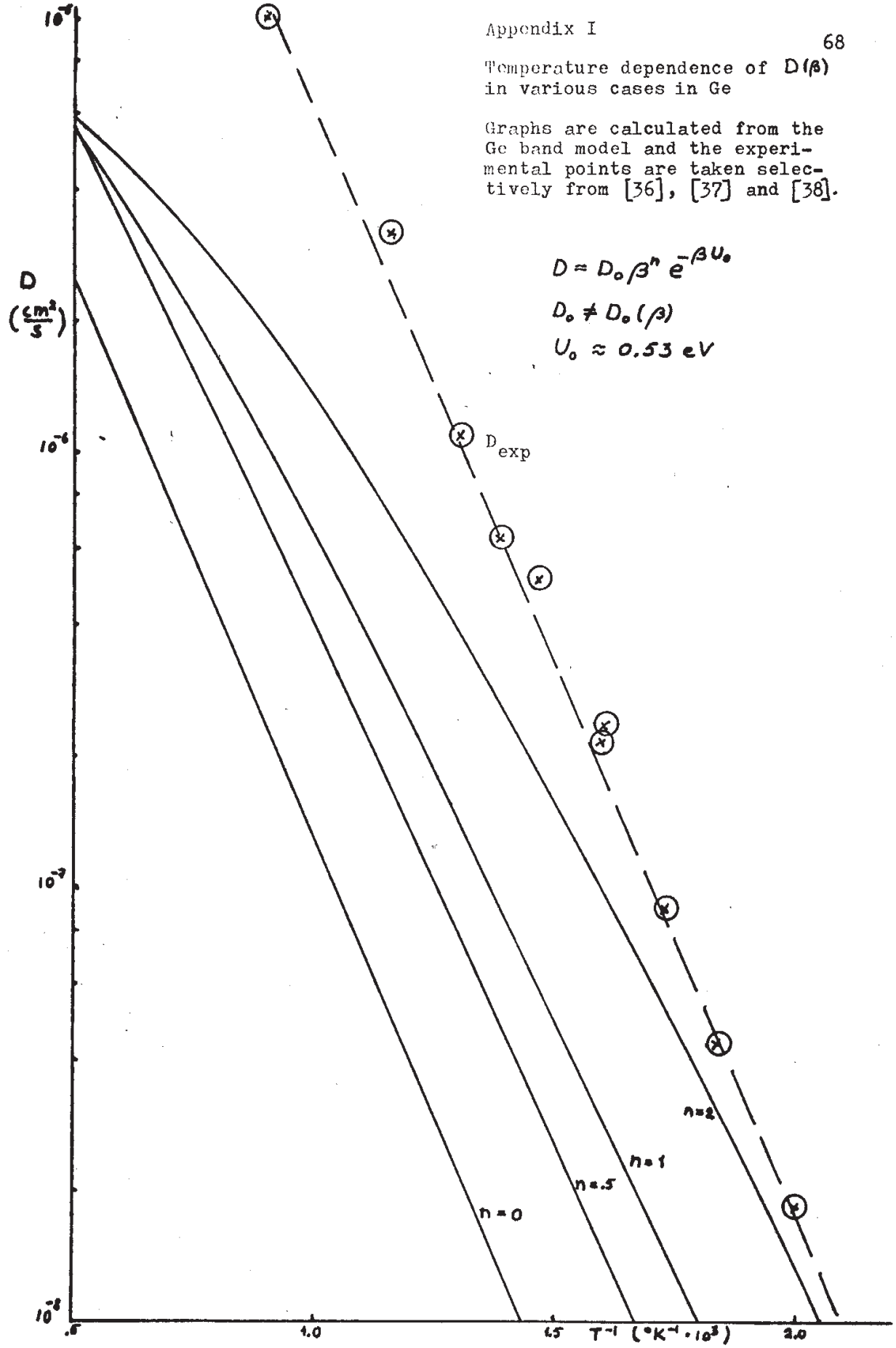

6. REFERENCES

[1] S. Glasstone, K. Laidler, H. Eyring, The Theory of Rate Processes.(McGraw-Hill, New York,1941)

[2] C.Wert, C. Zener, Phys. Rev. 76 1169 (1949)

[3] C. Zener, W. Shockley (Editor), Imperfections in Nearly Perfect Crystals.(Wiley,New York,1952)

[4] C. Wert, Phys. Rev. 79 601 (1950)

[5] G. Vineyard, J. Phys. Chem. Solids 3 121 (1957)

[6] S. Rice, Phys. Rev. 112 804 (1958)

[7] S. Chandrasekhar, Rev. Mod. Phys. 15 1 (1943)

[8] H. Glyde, Rev. Mod. Phys. 39 373 (1967)

[9] G. Nardelli, L. Reatto, Physica 31 541 (1965)

[10] P. Gosar, Il Nuovo Cimento 31 781 (1964)

[11] A. F. Andreev, I. M. Lifshitz, Sov. Phys. JETP 29 1107 (1969)

[12] J. Hetherington, Phys. Rev. 176 231 (1968)

[13] M. I. Klinger, Sov. Phys. Dokl. 13 1131 (1969)

[14] R. A. Guyer, L I. Zane, Phys. Rev. Lett. 24 660 (1970)

[15] M. I. Klinger, Rep. Prog. Phys. 31 225 (1968)

[16] C. P. Flynn, A. M. Stoneham, Phys. Rev. B1 3966 (1970)

[17] Yu. Kagan, L. A. Maksimov, Sov. Phys. JETP 38 307 (1974)

[18] Yu. Kagan, M. I. Klinger, J. Phys. C7 2791 (1974)

[19] M. I. Klinger, J. Phys. C8 2343 (1975)

[20] F. García-Moliner, Theory of Condensed Matter, Trieste Lectures, Trieste 1967, p. 229, IAEA (1968) Vienna

[21] D. Shaw, Atomic Diffusion in Semiconductors, p. 32,38, Editor D. Shaw, Plenum Press (1973)

[22] W. Jones, N. March, Theoretical Solid State Physics, vol. 1 chapters 1.9 and 1.11.4, Wiley (1973)

[23] M. I. Klinger, Sov. Phys. Dokl. 21 509 (1976)

[24] K. Weiser, Phys. Rev. 126 1427 (1962)

[25] J. Callaway, Energy Band Theory, chapter 1, Academic Press (1964)

[26] S. M. Hu, Atomic Diffusion in Semiconductors, p. 217, Editor D. Shaw, Wiley (1973)

[27] R. B. Dingle, Phil. Mag. 46 831 (1955)

[28] R. A. Swalin, J. Phys. Chem. Solids 23 153 (1962)

[29] L. Pauling, The Nature of the Chemical Bond, (2nd ed.) Cornell Press, Ithaca, New York (1940)

[30] D. P. Kennedy, Proc. IEEE (Ltrs) 57 1202 (1969)

[31] N. W. Ashcroft, N. D. Mermin, Solid state Physics, Holt, Rinehart and Winston (1976)

[32] B. Yavorsky, A. Detlaf, Handbook of Physics, p. 922, English transl. Mir Publ. (1975)

[33] R. A. Swalin, Atomic Diffusion in Semiconductors, p. 65, Editor D. Shaw, Plenum Press (1973)

[34] G. Kaye, T. Laby, Tables of Physical and Chemical Constants, Longman (1973)

[35] E. Gorham-Bergeron, Phys. Rev. Lett. 37 146 (1976)

[36] C. Fuller, J. Ditzenberger, Phys. Rev. 91 193 (1953)

[37] C. Fuller, J. Severiens, Phys. Rev. 96 21 (1954)

[38] B. Pratt, F. Friedman, J. Appl. Phys. 37 1893 (1966)

[39] Yu. Shaskov, I. Akimchenko, Dokl. Akad. Nauk. SSSR 128 937 (1959)

[40] E. M. Pell, Phys. Rev. 119 1014, 1222 (1960)

[41] E. M. Pell, J. Phys. Chem. Solids 3 77 (1957)

[42] J. H. Weiner, Phys. Rev. B14 4741 (1976)

[43] A. D. LeClaire, Phil. Mag. 14 1271 (1966)

[44] J. N. Mundy, L. W. Barr and F. A. Smith, Phil. Mag. 14 785 (1966)